FRONTIERS OF BIOGEOGRAPHY
The scientific journal of The International Biogeography Society

Frontiers of Biogeography 19, 2026, e150642 | DOI 10.21425/fob.19.150642

RESEARCH ARTICLE

The role of the climate niche in repeated abrupt tree declines and ecotone dynamics in the Appalachian Mountains during the Holocene

Bryan N. Shuman[1], Ivanka Stefanova[2], Ioana C. Stefanescu[1], Tessa Ray-Cozzens[1], Jonathan Johnson[3], David M. Nelson[3]

1 *Department of Geology and Geophysics, University of Wyoming, Laramie WY 82071, USA*
2 *Department of Earth and Environmental Sciences, University of Minnesota, Minneapolis, MN 55455, USA*
3 *Appalachian Laboratory, University of Maryland Center for Environmental Science, Frostburg MD 21532, USA*

Corresponding author: Bryan N. Shuman (bshuman@uwyo.edu)

Editors Janet Franklin
Received 19 February 2025 ♦ **Accepted** 24 November 2025 ♦ **Published** 18 February 2026

Abstract

Forests in eastern North American did not achieve a stable composition during the Holocene. Both prolonged and abrupt shifts in the distributions of tree species were common. Studying the dynamics involved can help anticipate the responsiveness of forest biogeography to climate change today. Here, we evaluate changes in two > 12,000-year fossil pollen stratigraphies from the Appalachian Plateaus Province, Pennsylvania. They show repeated episodes of forest turnover following the widespread collapse of hemlock (*Tsuga canadensis*) populations at ca. 5000 years before present (YBP), which locally coincided with severe drought and rapid warming of 1.1 °C (0.9–1.3 °C) indicated by lake-level changes and geochemical proxies. The subsequent vegetation changes from 5000-2500 YBP included abrupt declines in birch (*Betula* spp.) and beech (*Fagus grandifolia*) and a series of unique forest phases each lasting 300–500 years in association with unique combinations of temperature and moisture. Emergent communities included the resurgence of oak (*Quercus* spp.) and white pine (*Pinus strobus*), which had been important several thousand years earlier. Two oak maxima at 4800-4250 YBP and 3800-3200 YBP mark northward shifts in the northern-temperate forest ecotone known as the "Tension Zone" during the warm-dry phase that coincided with low hemlock abundance. The changes, like those elsewhere along the ecotone from Ontario to Massachusetts, differ from successional or stochastic dynamics that might have been expected after the hemlock decline. Instead, the forest histories included abrupt changes, short-lived communities and asynchronous changes across sites consistent with the interaction of: a) individualistic species' climate niches and b) multiple scales of climate variation.

Highlights

- Repeated episodes of abrupt change reveal the sensitivity of Appalachian forests to climate change during the past > 11,000 years.
- Two fossil pollen records from Pennsylvania show that the abrupt changes produced distinctive phases of forest composition lasting 300–500 years.
- An abrupt range-wide decline in hemlock (*Tsuga canadensis*) about 5000 years before present coincided locally with drought and rapid warming of ~ 1 °C.
- Additional abrupt declines in beech (*Fagus grandifolia*) and birch (*Betula* spp.) followed the hemlock decline and were followed, in turn, by increases in taxa like oak (*Quercus* spp.) and white pine (*Pinus strobus*) consistent with shifts in regional vegetation gradients and ecotones.
- The patterns of forest turnover differ from examples of post-disturbance succession, but conform with simulated interactions of climate change and species' climate niches.

Keywords

Abrupt change, Appalachian, ecotone, forest, Holocene, Pennsylvania, pollen, *Tsuga*

Introduction

Paradoxically, abrupt forest changes (< 500 yrs) were common during the ostensibly 'stable' climates of the Holocene Epoch of the past 11,700 years (Shuman et al. 2009; Seddon et al. 2015). Evaluating the processes that shaped these abrupt changes can help to anticipate future ecosystem outcomes of anthropogenic climate change (Williams et al. 2011; Jackson and Blois 2015). Fossil pollen stratigraphies from the northeast U.S. (Fig. 1) provide a particularly useful case because they document a rich sequence of forest changes, which developed in the context of millennial and centennial climate variability (Davis 1969; Watts 1979; Gaudreau and Webb 1985; Oswald et al. 2020). The variability induced continuous changes in forest communities consistent with definitions of a 'dynamic equilibrium' (Webb III 1986; Blonder et al. 2017): forest turnover was rapid compared to climate trends and yielded compositional changes that were quantitatively similar to those across geographic climate gradients today (Prentice et al. 1991; Shuman et al. 2019). However, the details of the stratigraphies also indicate centennial-scale variations, including abrupt tree declines (e.g. Davis (1981); Clifford and Booth (2015)), which may reflect the interactions between intrinsic forest processes like disturbance and succession and externally-driven responses to the regional climate history (Fuller 1998; Williams et al. 2011; Shuman et al. 2019). The short-lived changes also altered first-order biogeographic patterns such as the north-eastern U.S. forest ecotone, known as the 'Tension Zone,' between northern hardwoods and conifers (green-yellow in Fig. 1) and southern oak-hickory (*Quercus-Carya*) forests (tan in Fig. 1) (Cogbill et al. 2002; Thompson et al. 2013; Paciorek et al. 2016).

The north-eastern Tension Zone has a dynamic Holocene history related to climate changes, disturbance and species migration (Bernabo and Webb 1977; Fuller et al. 1998; Foster et al. 2002; Thompson et al. 2013; Oswald et al. 2018). Changes affecting the ecotone included a rapid, range-wide decline of the eastern hemlock (*Tsuga canadensis*) populations (yellow, Fig. 1). The decline at ca. 5000 years before present (YBP) has been well studied and debated and explanations for it range from disease to temperature shifts (Davis 1981; Allison et al. 1986; Calcote 2003; Foster et al. 2006; Booth et al. 2012; Shuman et al. 2023). Additional, potentially related, centennial-scale variations in forest composition followed the hemlock decline at Tension Zone sites from Massachusetts to Ontario (Fuller 1998; Oswald et al. 2007; Oswald et al. 2018). Hypotheses about the causes of these forest changes have not been thoroughly examined.

First, the range-wide hemlock decline, regardless of its cause, may have initiated successional dynamics across the region, which would appear as distinct centennial-scale forest phases in Holocene pollen records (Fuller 1998). Such phases may also represent independent impacts of forest diseases (Allison et al. 1986), insect outbreaks (Anderson et al. 1986; Bhiry and Filion 1996), extreme weather events (Foster and Boose 1992; Pederson et al. 2014) and human use of wildfire (Maenza-Gmelch 1997; Nowacki and Abrams 2008; Nowacki and Abrams 2015). Evidence of such disturbances is often not present (Foster et al. 2006; Oswald et al. 2016; Oswald et al. 2020), but sequences of compounded large disturbances could have generated centennial-scale forest phases by triggering asynchronous abrupt declines

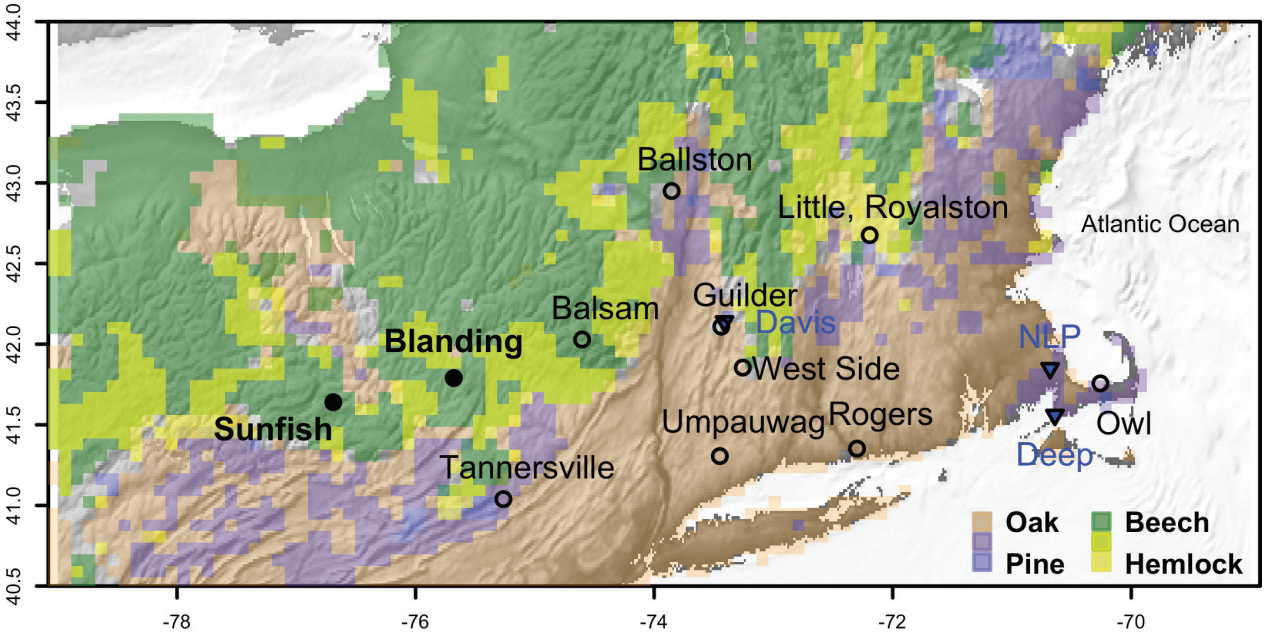

Figure 1. Historic distributions of forests with > 20% oak (tan), pine (blue), beech (green) or hemlock trees (yellow) in the northeast U.S. Locations of fossil pollen (circles) and lake level (blue triangles) study sites discussed here are also shown. Intermediate colours (purple, light green) represent mixtures of taxa. The focal study sites are shown in bold with filled black circles. NLP refers to New Long Pond. Tree distribution data from Paciorek et al. (2016).

with the most sensitive taxa (e.g. hemlock) declining immediately, followed later by other taxa stressed by previous events (Paine et al. 1998; Turner et al. 2019). Large disturbances in sequence can, in this way, disrupt the emergence of a 'steady state' in the regional forest mosaic (Baker 1989; Turner et al. 1993). If so, the changes should be inconsistently related to climate, comparable to known examples of disturbance and succession and spatially heterogeneous like disturbance.

Alternatively, the centennial changes in forest composition may represent ecological 'random walks' driven by neutral ecological dynamics that allow tree populations to rise and fall as a result of temporally autocorrelated demographic processes (Clark and McLachlan 2003; Blaauw et al. 2010; Ramiadantsoa et al. 2019). Stochastic extreme events and autoregressive population processes likely create complex forest trajectories at forest stand scales, which may scale up to produce centennial-scale regional outcomes contingent on the sequence of events rather than closely tracking the shifting mean climate (Jackson et al. 2009; Pederson et al. 2014; Ramiadantsoa et al. 2019). If so, the changes should show no predictable sequence and weak correlations across broad geographic scales (Clark and McLachlan 2003; Blaauw et al. 2010).

Finally, the forest changes could represent the interaction between species' climate niches (Prentice et al. 1991; Williams et al. 2006) and centennial-to-millennial climate fluctuations (Yu et al. 1997; Foster et al. 2006; Li et al. 2007; Marsicek et al. 2013; Shuman and Burrell 2017; Shuman et al. 2019; Shuman et al. 2023; Stefanescu et al. 2023). Centennial forest variability, even including abrupt tree declines, could arise at the scale of landscapes (pollen source areas) from the dynamic equilibrium between the fluctuating regional climate and the shifting mosaic of forest stands with different edaphic, disturbance and population histories, i.e. the mean outcome of many individual forest stands may closely track the mean climate trends as determined by species climate niches (Webb III 1986; Prentice et al. 1991; Shuman et al. 2019). Time scale matters, however (Fastovich et al. 2025). Over decades, locally-adapted population responses to climate may be muted and vary geographically (Perret et al. 2024), but over centuries, shifts in populations and genotypes can converge on outcomes consistent with species' range-wide climate relationships (Davis and Shaw 2001; Blois et al. 2013; Shuman et al. 2019). Even at intermediate timescales, transient vegetation changes may trend towards equilibria between tree abundances and climate, even if they do not fully achieve it (Webb III 1986). In this case, the changes should show spatiotemporal patterns consistent with independent palaeoclimate records and form sequences consistent with climate niches today.

Here, we consider the relevance of these end-member hypotheses to centennial-scale forest variation and find evidence that climate-niche interactions shaped repeated abrupt tree declines near the Tension Zone in the Appalachian Plateau Province of Pennsylvania. We focus on forest changes from 5000-2500 YBP when the hemlock decline and related changes took place (Davis 1981; Fuller 1998; Foster et al. 2006; Shuman et al. 2023). For context, we use simple one-dimensional heuristic simulations to demonstrate changes that could have arisen from the interaction of species climate niches and lagged responses to Holocene climate variability. We then identify the patterns of forest turnover in two new fossil pollen stratigraphies, which we compare with palaeoclimate records and examples of known successional changes.

Study sites

The two study sites, Blanding Lake and Sunfish Pond, sit within the highlands of Pennsylvania (Fig. 1). Both are located near the Tension Zone in forests populated since at least the 18th century by hemlock, beech (*Fagus grandifolia*), multiple maple species (*Acer* spp.) and various birches (*Betula* spp.) (Cogbill et al. 2002; Thompson et al. 2013; Paciorek et al. 2016). Blanding Lake (41.798°N, 75.676°W, 454 m elevation, 4.8 ha, 555 cm maximum water depth) is one of many similar-sized lakes located amidst rolling hills and steep-sided valleys of the Delaware-Neversink Highlands in Susquehanna Co., Pennsylvania (Sevon 2000). July temperatures at the lake currently (1991–2020 CE normals) have a mean of 20.0 °C, while January has a mean of -5.7 °C; mean annual temperature and precipitation equal 7.5 °C and 1175 mm, respectively (PRISM Climate Group 2022). The landscape surrounding Blanding Lake contains a nearly even mix of managed deciduous forests and cleared agricultural areas. The lake itself sits within a small primarily forested watershed (45 ha) defined by hills and ridges reaching to ~ 500 m elevation above sea level. Previous work showed that the lake level fluctuated repeatedly since the lake's formation ca. 15,000 YBP with low water episodes from ca. 12,000-9000, 5500-3800 and 2800-2000 YBP (Shuman and Burrell 2017).

Sunfish Pond (41.644°N, 76.697°W, 635 m elevation, 11 ha, 585 cm maximum depth) is a glacially formed lake, located on a ridge crest in the Allegheny Mountains in Bradford County, Pennsylvania. The 1.1 km^2 watershed drains an area of low relief on top of LeRoy Mountain within the Glaciated High Plateau Region (Wood et al. 1911; Sevon 2000). Steep, northwest facing mountain slopes north of the lake descend > 300 m in elevation in < 2 km to reach the Low Plateau region crossed by the Susquehanna River. European settlement of Bradford County around Sunfish Pond dates to 1760 CE, but human population density remained low near the lake allowing the creation of Pennsylvania State Game Management Lands to conserve the lake watershed and surrounding areas as forest (Wood et al. 1911).

The local climate is similar to that at Blanding Lake with mean annual, July and January temperatures of 7.5, 19.9 and -5.5 °C, respectively, and mean annual precipitation

of 1140 mm (PRISM Climate Group 2022). However, anti-phased precipitation variations at Sunfish Pond and Blanding Lake can result because a rainshadow extends behind the eastern Appalachian ridges between the two lakes (Brady and Waldstreicher 2001; PRISM Climate Group 2022) and the North Atlantic Oscillation and other dynamics alter the inland extent of storm tracks and cyclogenesis (Bradbury et al. 2003; Chartrand and Pausata 2020). Sunfish Pond experienced a history of Holocene water-level changes that differed in detail from that at Blanding Lake, including low-water phases at ca. 10,000–8000 and 5800-3800 YBP (Ray-Cozzens 2022).

Soils also differentiate the two lakes. The Volusia-Morris soil series, a group of deep, moderately drained soils in loamy till, surround Blanding Lake (Reber 1973), which occupies a depression within the Pleistocene Orlean Till over sandstones of the Devonian Catskill Formation (Berg et al. 1980; Sevon and Braun 1997; Braun 2004). At Sunfish Pond, however, only thin glacial till and scattered glacial erratics cover the underlying bedrock, composed of the Pottsville Formation, a grey sandstone and conglomerate (Myers 1954). The local Lordstown soil series is composed of well-drained soils formed in till and cryoturbated fragments of the underlying siltstone and sandstone (USDA Natural Resources Conservation Service 2016).

Materials and methods

Simulations

Simple models can focus on specific processes and clarify the implications of a hypothesis even when they do not capture the details critical for specific ecological predictions (e.g. Davis and Botkin (1985); Turner et al. (1993); Blaauw et al. (2010); Calder and Shuman (2017); Ramiadantsoa et al. (2019)). Here, we simulate three idealised taxa and their dynamic responses to decadal to multi-millennial climate variations. We do so to demonstrate how species' climate niches might shape centennial-scale vegetation responses to climate at the landscape scale. Most niches exist in multiple dimensions defined by seasonal temperatures and moisture availability (Williams et al. 2006), but for our purposes, we simulate a simplified niche for our idealised taxa based on a single arbitrary 'climate' index (Fig. 2A–C). Similar models including multiple driving variables produce comparable outcomes (Blaauw et al. 2010).

The underlying premise derives from theory and observations about climatic niches: processes from regeneration to competition define a unimodal climatic optimum for most tree species (Grubb 1977; Prentice et al. 1991; Peterson et al. 2011). The interaction of the suite of niche-defining processes with climate variations drives fluctuations in tree abundances consistent with the emergent unimodal climate optima. However, processes like persistence of mature individuals, growth of new recruits and succession can delay the climate-driven expectations; these lagging processes create transient communities that emerge on century scales as forests chase a dynamic equilibrium with the non-stationary climate (Webb III 1986).

Our dynamic equilibrium-niche model representing these concepts includes two key equations, calculated in R (R Core Development Team 2022). First, each pseudo-species has an abundance that is (in this simplified model) deterministically based on the climate index at time T (C_t), such that, between two limits (C_{min}, C_{max}), the abundance represents a single sine wave with a fixed mode (C_{mode}) and breadth ($C_{breadth}$):

$$\text{For} \quad C_t > C_{min} \quad \text{and} \quad C_t < C_{max}:$$

$$A_t = \sin\left(0.5 + \left(\left(C_t - C_{coode}\right)/C_{breadth}\right)\right) \qquad (1)$$

When the value of the climate at any point in time (C_t) falls outside of the two limits, the abundance (A_t) becomes zero.

Second, to account for the lagging changes, we apply the concept of an 'e-folding' response time (λ), which represents the amount of time for ~ 63% of the response to develop (Webb III 1986):

$$A_T = A_t + (A_{T-1} - A_t) * \exp(-t/\lambda) \qquad (2)$$

Here, A_T and A_{T-1} represent the actual abundances at time T and T-1 and A_t represents the potential abundance determined by the niche at time T from equation 1. The time step of the model (t) used here is 20 years. We use 75 years for λ to approximate successional time scales (i.e. the duration of the first 63% of the changes) in Appalachian deciduous forests. As near-equilibrium (99% of the potential change) would require five e-folding times, transient dynamics dominate over timescales of up to 375 years (see also Fastovich et al. (2025)).

We apply the model to three pseudo-species with different climatic modes spread across a climate gradient spanning the magnitude of a synthetic 8000-year climate trend. We added a millennial oscillation and a second, smaller multi-century oscillation (i.e. two sine waves) to the trend (black line, Fig. 2D), as well as stochastic decadal variability (black lines, Fig. 2E, F). For comparison, we generated a first simulation without the stochastic decadal variability and then two different simulations representing different 'sites' with the same mean climate trend and oscillations, but different decadal variability (black and red lines, Fig. 2E, F). The stochastic decadal variability primarily represents atmospheric variability, but could be considered to include site-level microclimate variations shaped by local disturbances and other forest ecosystem processes. Although the decadal variability is randomly drawn from a normal distribution, the simulated species responses are entirely deterministic following equations 1 and 2. The model, thus, represents an extreme, simplified form of the dynamic equilibrium-niche model, which we contrast with the two new pollen records from Sunfish Pond and Blanding Lake.

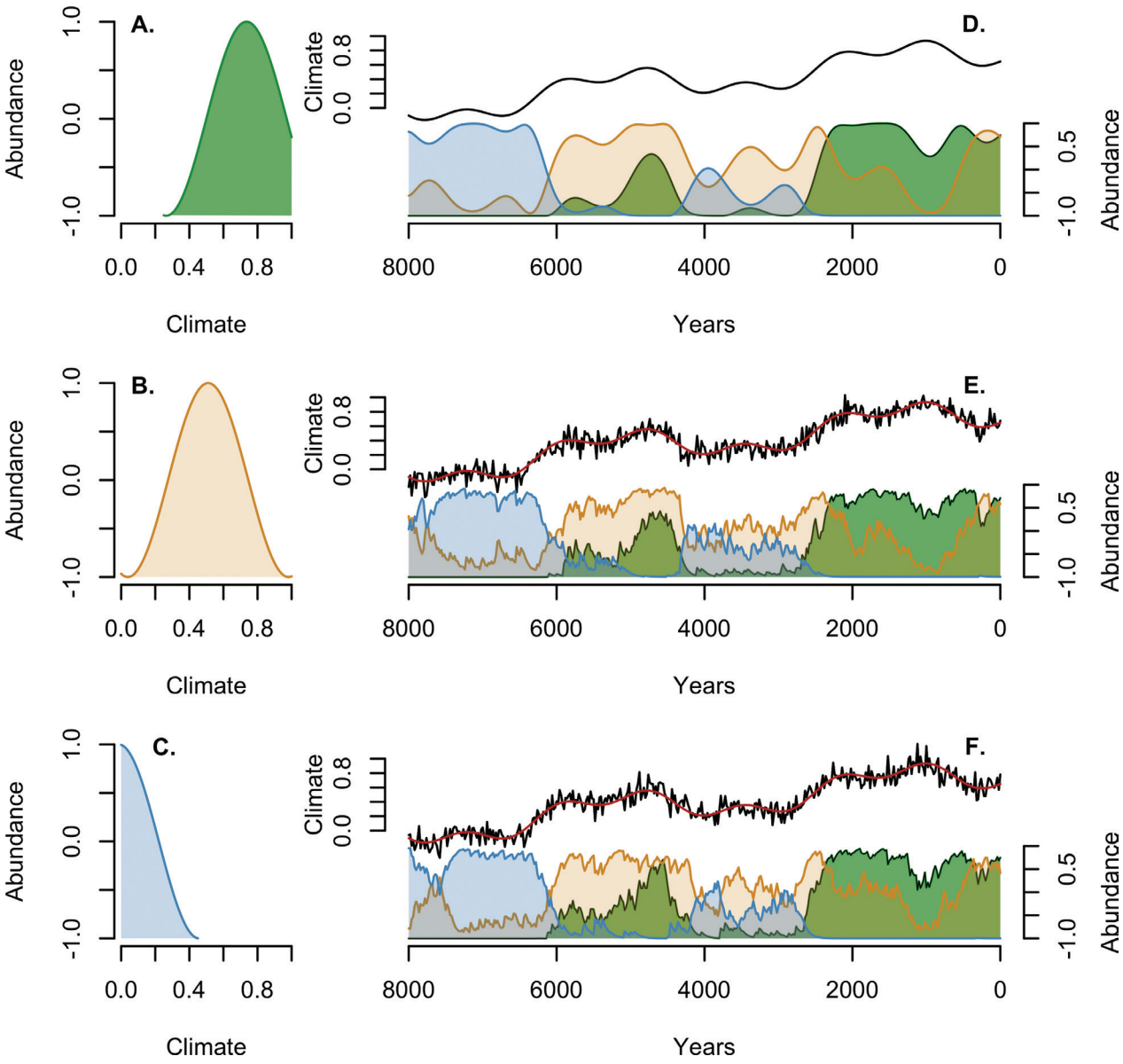

Figure 2. Simulations of the 8000-year histories of three pseudo-species (**A–C**), based on deterministic responses to synthetic climate histories (**D–F**). The responses are governed by the pseudo-species' sine-form climate response curves (**A–C**). Black lines in **D–F** represent the 'climate' history used to drive each set of calculations; red lines in **E, F** show the trend and oscillations (same as in **D**) underlying the synthetic histories, which also include two different sets of stochastic decadal variability at the two different 'sites' represented in **E, F**. Coloured shading shows outcomes from equations 1 and 2 for each pseudo-species: **A** (green), **B** (tan) and **C** (blue). Time progresses from 8000 years to year 0 to parallel the Holocene datasets.

Sediment core analyses

Cores were collected from the deepest point within each lake in 2015 from a floating platform using a hand-driven piston corer. Core sections were retrieved in sequential sections through the entire thickness of lake sediment in 1-m long, 70-mm diameter plastic tubes. The sections were refrigerated upon arrival at the University of Wyoming where they were split and sub-sampled in contiguous 1-cm intervals. All sub-samples were analysed for loss-on-ignition (LOI) at 550 °C for 2 hrs to estimate organic content (Shuman 2003).

Core chronologies were developed by sieving sub-samples to obtain macroscopic charcoal fragments for radiocarbon analyses. However, the Sunfish Pond core contained insufficient charcoal and 1–3 cm^3 bulk sediment samples were analysed instead because the sediment was organic-rich and contained no carbonates, which are also absent from the watershed. Charcoal samples were analysed by the W. M. Keck Carbon Cycle Accelerator Mass Spectrometer Facility at the University of California, Irvine and bulk sediment samples by National Ocean Sciences Accelerator Mass Spectrometry at the Woods Hole Oceanographic Institution. Resulting radiocarbon ages were calibrated using Intcal20 (Reimer et al. 2020) and age-depth models were generated using bchron (Haslett and Parnell 2008; Parnell et al. 2008). Resulting sample ages were compared across the two sites, to assess the quality of bulk sediment ages and detect outliers, by contrasting

the timing of regionally significant features in their birch (*Betula*) and hemlock (*Tsuga*) pollen stratigraphies.

Pollen was processed and counted from selected sub-samples using standard techniques (Fægri et al. 1992). Samples were initially selected in each core at 15–20 cm intervals to provide ~ 300-yr sample spacing, based on the chronologies. Additional subsamples were added to the Sunfish Pond core from 8000-2800 YBP to increase temporal resolution to < 130 yrs between samples. The samples were processed at the University of Wisconsin-Madison and then mounted on slides and counted under 40x magnification at LacCore at the University of Minnesota. On average, 500 individual palynomorphs were counted from each sample. Pollen percentages were calculated from the sum of terrestrial pollen types.

Constrained cluster analysis (CONISS) (Grimm 1987) was used to determine the location of major changes in the pollen assemblages within each stratigraphy; stratigraphically adjacent clusters were determined using Bray-Curtis dissimilarity amongst the percentages of taxa with > 2% representation. The analysis was conducted using *chclust* in the *rioja* package in R and significance of the breaks were tested using *bstick* and plotted using *riojaPlot* (R Core Development Team 2022; Juggins 2024). Low-frequency variations in the time series of individual taxa were estimated using the *loess* function in base R to create a 5000-yr moving-window smoother.

To constrain the local temperature history for comparison with the pollen stratigraphies, lake-level histories and regional temperature reconstructions, temperature-sensitive lipids from the membranes of bacterial cells, known as branched glycerol dialkyl glyercerol tetraethers (brGDGTs), were extracted and analysed in the same samples as the pollen from Blanding Lake. Extraction and analysis of brGDGTs at the University of Wyoming followed the protocols of Stefanescu et al. (2021, 2023), consistent with standardised methods (e.g. Hopmans et al. (2016); Raberg et al. (2021)) and validated as part of a large inter-lab comparison (De Jonge et al. 2024). The free lipid component of freeze-dried sediment was extracted using a Dionex Accelerated Solvent Extractor (Stefanescu et al. 2023) and then analysed by utilising an Agilent 1200 HPLC and Thermo Orbitrap (Q-Extractive-HF X) mass spectrometer with an Atmospheric Pressure Chemical Ionisation (APCI) source. Mean temperature above freezing (MAF) was reconstructed from the brGDGT abundances using calibrations, based on both the MBT'5me index (Martínez-Sosa et al. 2021) and the sub-set of brGDGTs expressing temperature-related methylation (the 'meth set'; Raberg et al. (2021)).

Results

Simulations

Our simulations demonstrate how several features of Holocene forest histories could develop from the interaction of species' climate niches and multiple scales of climate variability (Fig. 2):

1. Sequences of abrupt tree declines (and increases), which can be at least as fast as the driving climate forcing;
2. Development and repetition of short-lived phases dominated by different taxa; and
3. Differences amongst sites despite consistent, underlying low-frequency changes.

In the simulations, taxon A dominates at high 'climate' index values (green, Fig. 2A), taxon B at intermediate values (tan, Fig. 2B) and taxon C at low values (blue, Fig. 2C). Consequently, a long-term trend causes taxon C (blue) to dominate for the first two millennia, followed by taxon B (tan) and then finally, taxon A (green). Additional millennial and centennial fluctuations in the abundance of the three taxa also interrupt and, at times, reverse the major vegetation phases. For example, taxon A (green) briefly increases from ca. 6000–4500 years, declines from ca. 4500–2500 years and then becomes dominant in the last 2500 years (Fig. 2D). Each pseudo-species also has a large decline between 6500–4000 years: taxon C (blue) at ca. 6500 years, taxon A (green) at ca. 4500 years and then taxon B (tan) at ca. 4000 years (Fig. 2D).

The stochastic decadal 'climate' variability creates two additional effects (Fig. 2E, F). First, abrupt declines and increases, such as exist in many pollen records (e.g. Booth et al. (2012); Schlenker et al. (2024)), emerge when the added decadal variability interacts with the asymptote of each response curve to accentuate the rates of change, such as when taxon B collapses rapidly at ca. 4500–4000 years (tan, Fig. 2E). Second, because the decadal variability differs between the two stochastic experiments, the timing of abrupt changes and even the presence (or not) of short-lived peaks in the abundance of the taxa, differs (Fig. 2E, F). For example, at the first experimental 'site', taxon A (green) and taxon B (tan) both decline abruptly when taxon C (blue) increases rapidly at ca. 4500 years (Fig. 2E). At the second 'site' (Fig. 2F), however, taxon A (green) declines faster than B (tan) and faster than the underlying 'climate' change (red line in Fig. 2F), consistent with some observations of vegetation changes leading their climatic driver (Williams et al. 2002; Booth et al. 2012). Large disturbances, ecological random walks and palaeoecological sampling errors could potentially produce similar abrupt changes and stochastic differences amongst sites (Shane 1989; Blaauw et al. 2010; Calder and Shuman 2017), but the simulations demonstrate that deterministic responses to climate variations can also produce such features. If they did, pollen records showing these features should correlate with climate history in a manner consistent with the underlying climate niches.

Sediment cores and chronologies

To evaluate these expectations and the history of the Tension Zone, sediment cores that are 930- and 785-cm long were collected from Blanding Lake and Sunfish Pond, respectively.

Nine calibrated radiocarbon ages (Table 1) form the basis of the Blanding Lake chronology; a tenth date

Table 1. Radiocarbon ages from the Blanding Lake and Sunfish Pond cores.

		Depth	Thickness			^{14}C age	Uncertainty		Calibrated age range		
Lake	Core	(top cm)	(cm)	Material	Lab number	(YBP)	(yr)	Accepted	5%	Median	95%
Blanding Lake	555	546	1		Core top	-65	1				
	555	619	2	charcoal	UCI-190318	625	45		550	601	658
	555	679	2	charcoal	UCI-190319	2225	35		2159	2228	2320
	555	796	2	charcoal	UCI-190320	3450	70		3578	3716	3858
	555	873	1	charcoal	UCI-190321	4280	20		4837	4847	4858
	555	913	1	charcoal	UCI-190322	4410	20		4891	4986	5036
	555	1025	2	charcoal	UCI-190323	16300	80	No	19534	19670	19852
	555	1086	1	charcoal	UCI-190324	7230	130		7842	8059	8292
	555	1122	1	charcoal	UCI-190325	7925	50		8631	8765	8963
	555	1198	2	charcoal	UCI-190326	8950	60		9913	10057	10206
	555	1283	1	charcoal	UCI-190327	12080	45		13809	13930	14038
Sunfish Pond	585B	585	1		Core top	-65	1		-67	-65	-64
	585B	671	1	charcoal	OS-127540	650	20		563	588	657
	585B	766	1	bulk sediment	OS-161249	2940	20		3011	3102	3159
	585B	796	1	bulk sediment	OS-161250	3870	25		4187	4304	4397
	585B	812	1	bulk sediment	OS-161251	4650	30	No	5320	5404	5456
	585B	838	1	charcoal	OS-127541	6520	65	No	7317	7427	7549
	585B	915	2	bulk sediment	OS-161275	5710	25		6419	6488	6585
	585B	962	1	bulk sediment	OS-127542	6840	70		7587	7676	7814
	585B	1060	1	bulk sediment	OS-127543	9190	110		10208	10377	10602
	585B	1060	1	bulk sediment	OS-127544	9330	110		10290	10533	10941
	585B	1108	1	bulk sediment	OS-161276	1130	15	No	976	1014	1060
	585B	1215	1	bulk sediment	OS-127545	15650	280	No	18387	18962	19478
	585B	1360	1	bulk sediment	OS-127546	38600	5500	No	34290	42452	52388

from the centre of the core (> 19,000 YBP) appears out of sequence (Fig. 3A). All ages derive from macroscopic charcoal. The bchron chronology provides regionally consistent ages of two widespread biostratigraphic features: 1) a peak in birch pollen percentages of > 30% at 12,500 YBP (13,520-10,900 YBP, 95% C.I.), which is widely documented (Gaudreau and Webb 1985 Mayle et al. 1993) and typically dates to 13,000-12,500 YBP (Shuman et al. 2009) and 2) the mid-point of the mid-Holocene hemlock decline from 27% to 8% at 5050 YBP (5640-4950 YBP, 95% C.I.), which compares well with regional age estimates of 5280 ± 180 YBP (Shuman et al. 2009) and 5025 YBP (5160-4895 YBP, 95% C.I., Booth et al. (2012)).

The Sunfish Pond chronology has several complications. Six calibrated radiocarbon ages were accepted for the final bchron chronology (Fig. 3B), but five additional ages were rejected either because they were out of stratigraphic position or because they created old, regionally inconsistent ages for the late-Pleistocene birch peak (blue lines, Fig. 3) and the mid-Holocene hemlock decline (green lines, Fig. 3). All, but one, of the accepted ages derive from bulk sediment; the youngest age derives from macroscopic charcoal. The rejected ages have the same mix of bulk sediment (4) and charcoal (1) ages. The final chronology included assigning the age of the early birch peak from Blanding Lake in place of the oldest radiocarbon ages because these two bulk ages of 19,100 and 42,500 YBP derive from the inorganic portion of the core and would cause the birch peak to have an unrealistically old age of ~ 14,000 YBP (Fig. 3B).

In the mid-Holocene, a bulk sediment age of 5400 YBP was also rejected (Fig. 3B) because it caused the hemlock decline to have an age of > 5700 YBP, which is > 500 years older than the decline at nearly all sites in the northeast U.S. (Shuman et al. 2009; Booth et al. 2012). The 5400 YBP age derives from a sandy interval of the core and could include re-worked material. An adjacent 7400 YBP charcoal age also appears to indicate the presence of old carbon; removing these ages places the hemlock decline at 5070 YBP (5960-4490 YBP, 95% C.I.)

Pollen stratigraphies

The Blanding Lake and Sunfish Pond pollen stratigraphies track patterns of vegetation change consistent with those expected in the region (Watts 1979; Barnosky et al. 1988; Oswald et al. 2007). At both lakes, conifers dominate the earliest portion of the record (Figs 4, 5), including in association with: 1) the regionally recognisable birch peak during the Younger Dryas (YD) chronozone (Gaudreau and Webb 1985: Barnosky et al. 1988: Peteet et al. 1990: Mayle et al. 1993) and 2) the subsequent phase when white pine (*P. strobus*) increased to > 40%, which is typical of the early Holocene in the region (Watts 1979; Shuman et al. 2009).

After ca. 10,000 YBP, different combinations of birch, beech, hemlock and oak dominate the pollen records along with pulses of white pine, hickory, ironwood (*Ostyra* and *Carpinus*), sugar maple (*Acer saccharum*) and chestnut (*Castanea*) (Figs 4, 5). Chestnut, birch, hemlock and diploxylon pines (*P. banksansia*, *P. resinosa* and *P. rigida*)

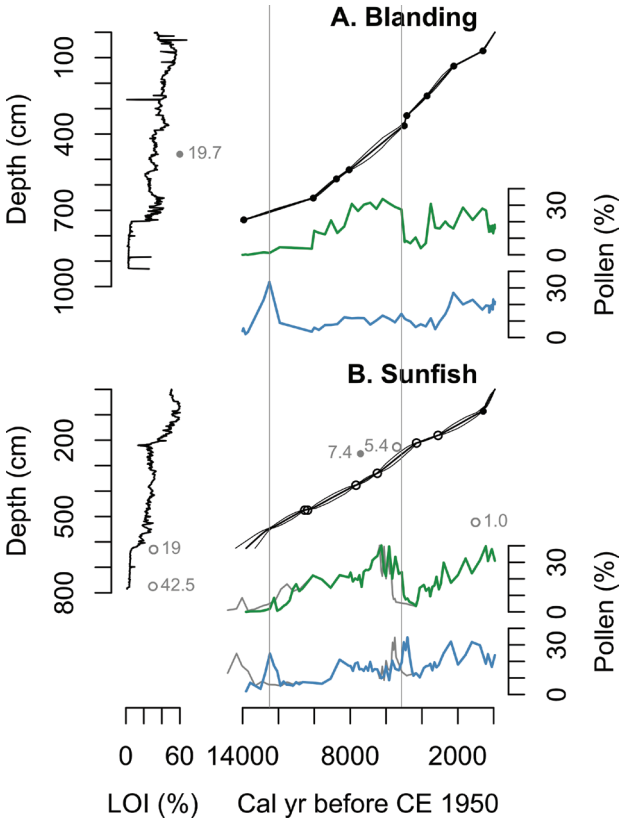

Figure 3. Age-depth relationships, calibrated radiocarbon dates, loss-on-ignition (LOI) profiles of the lake cores. Data are plotted by depth below the top of each core and hemlock (green) and birch (blue) pollen percentages by age for: **A.** Blanding Lake; **B.** Sunfish Pond. Closed circles indicate radiocarbon ages based on charcoal; open circles indicate ages derived from bulk sediment. Grey symbols indicate rejected ages and grey hemlock and birch pollen percentage lines represent the chronology with rejected ages included. Vertical lines mark the Younger Dryas-aged birch peak and the mid-Holocene hemlock decline. Black lines show the median and 95% range of sample ages estimated using bchron.

are all slightly more abundant at Sunfish Pond than at Blanding Lake. Additionally, pollen types representative of European land clearance (*Ambrosia*, *Rumex* and Poaceae) appear in the upper 50 cm at Blanding Lake (Fig. 4), but are not important at Sunfish Pond where historic land clearance was limited (Fig. 5).

Mid-Holocene variability

During the mid-to-late Holocene (5000-2500 YBP), sequences of short-lived (millennial-to-centennial) phases of distinct composition developed at both lakes, beginning with the hemlock decline. In both records, the phases included a sequence of maxima in the percentages of beech (> 30%), then oak (> 35%) and then white pine pollen (> 15%), as well as in minor types such as sugar maple (4–7%), hickory (> 2%), ironwood (3–4%) and chestnut (2–5%).

At Blanding Lake, low hemlock abundance after 5000 YBP coincided with: 1) the highest abundance (> 30%) of beech; 2) renewed high abundance (> 25%) of oak and 3) a modest increase in white pine (> 10%) after several millennia of near absence (Fig. 4). A series of short-lived peaks in abundance included oak at 4070 YBP, renewed hemlock (> 30%) at 3510 YBP, white pine (> 20% at 3260 YBP) and then oak (> 25%) again at 3250-3010 YBP. By 2500 YBP, oak and pine pollen percentages declined as birch pollen percentages rose to > 25%.

At Sunfish Pond, a similar mid-Holocene sequence of beech, oak and white pine also followed the hemlock decline (Figs 5, 6). Important patterns include:

1. maximum beech and birch pollen percentages (28–35%) from 5070-4810 YBP;
2. near-zero minima in white pine, ironwood and chestnut pollen percentages at the same time, even though they had briefly risen to 2–5%, respectively before 5070 YBP;
3. an abrupt transition from beech and birch to oak and hickory by 4620 YBP; and
4. an abrupt transition from oak and hickory to white pine and renewed hemlock by 4240 YBP (Fig. 6).

The Sunfish Pond stratigraphy includes both low-frequency, millennial-scale maxima and multi-century peaks that depart from the slow trends (Fig. 6). Low-frequency maxima represented by loess smoothers include broad maxima in oak (4810-3300 YBP), hickory (4910-3300 YBP), ironwood (4470-3420 YBP) and then white pine and chestnut (4690-2790 YBP). The superimposed multi-century peaks produced five distinct phases (Fig. 6): 1) birch and beech (5100-4800 YBP); 2) oak, hickory and chestnut (4800-4250 YBP); 3) white pine, hemlock and ironwood (4250-3800 YBP); 4) oak and white pine (3800-3200 YBP) and 5) chestnut (3200-2800 YBP).

Comparison with temperature and moisture histories

The major features of the two pollen records correspond with a series of climate changes indicated by the lake-level reconstructions (Shuman and Burrell 2017; Ray-Cozzens 2022), regional temperatures inferred from other pollen records (Shuman 2024) and the brGDGTs from Blanding Lake (Fig. 7). For example, hemlock pollen percentages correlated with the lake-level histories since 11,000 YBP (Pearson's product moment correlations, r = 0.45 and 0.37 at Blanding and Sunfish, respectively). At both lakes, the hemlock decline coincided with a pronounced drop in water levels by 4800 YBP. Hemlock's history differed, however, between sites according to their hydrologic differences. Hemlock increased at Sunfish during high water from 11,700-10,000 YBP (vertical grey bar, Fig. 7A) before it increased at Blanding, which experienced low water until ca. 10,000 YBP (vertical grey bar, Fig. 7B); these early-Holocene water level differences also correspond with higher white pine and lower oak pollen percentages before 10,000 YBP at Blanding (drier)

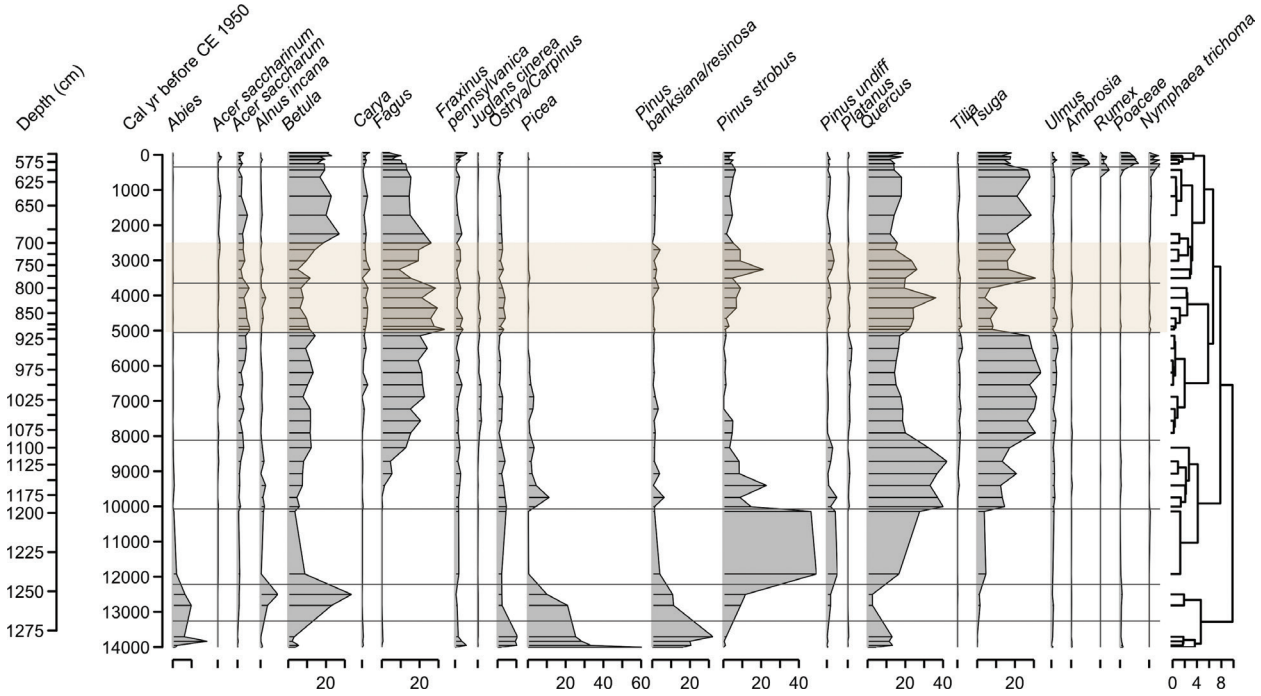

Figure 4. Summary pollen percentages from Blanding Lake. Horizontal lines represent the significant breaks (zones), based on the Bray-Curtis CONISS clustering at right. Tan shading highlights the interval from 5000-2500 YBP. Depths represent depth below the water surface. Taxa shown have a total sum of percentages across all samples that exceeds 20%.

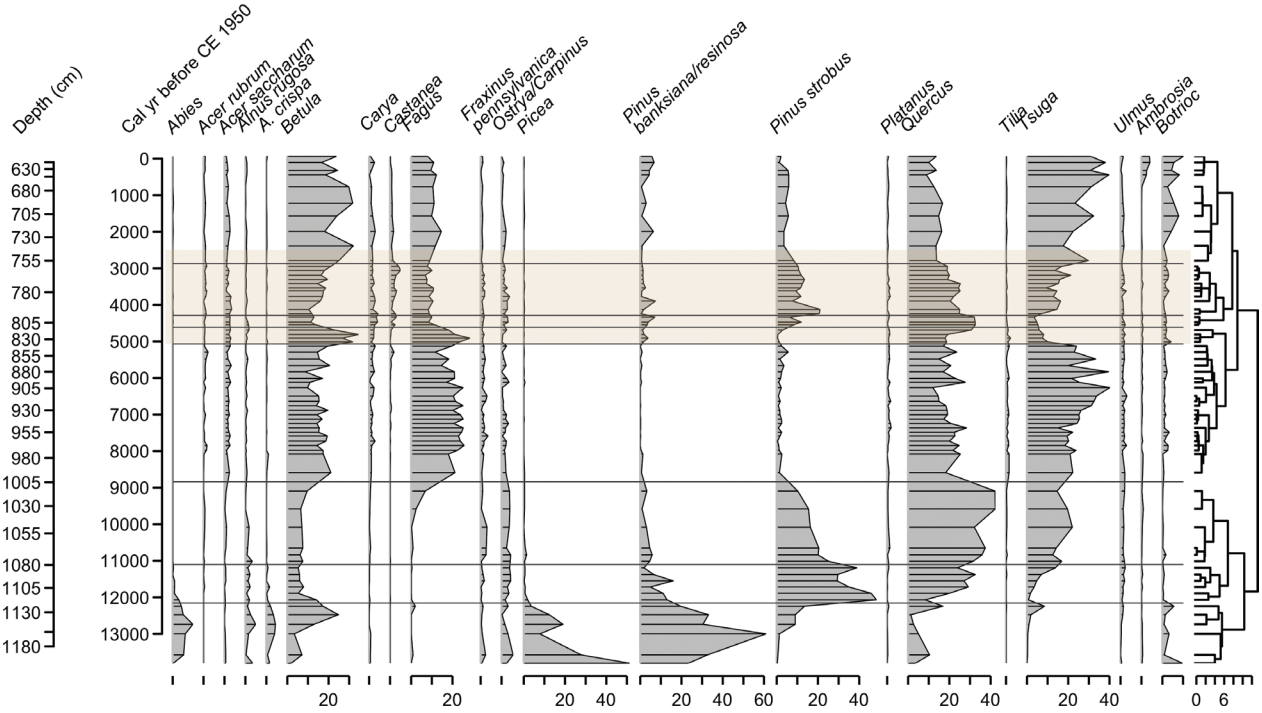

Figure 5. Summary pollen percentages for Sunfish Pond. Horizontal lines represent the significant breaks (zones), based on the Bray-Curtis CONISS clustering at right. Tan shading highlights the interval from 5000-2500 YBP. Taxa shown have a total sum of percentages across all samples that exceeds 20%.

than at Sunfish (wetter; bottom row, Fig. 7). Hemlock pollen percentages rose to > 30% by 8000 YBP at Blanding, but not until after 7000 YBP at Sunfish where water levels rose later. Finally, short-lived peaks during the post-decline recovery of hemlock also track the site-specific moisture histories with a more progressive recovery at Sunfish than Blanding (Fig. 7).

Temperatures inferred from the brGDGTs from Blanding Lake (red lines, Fig. 7B) correlate with a pollen-inferred temperature reconstruction predicated on vegetation responses to temperature across mid-latitude eastern North America (Shuman 2024) (grey lines, top row, Fig. 7); Pearson's product moment correlation, r, equals 0.51 (0.31–

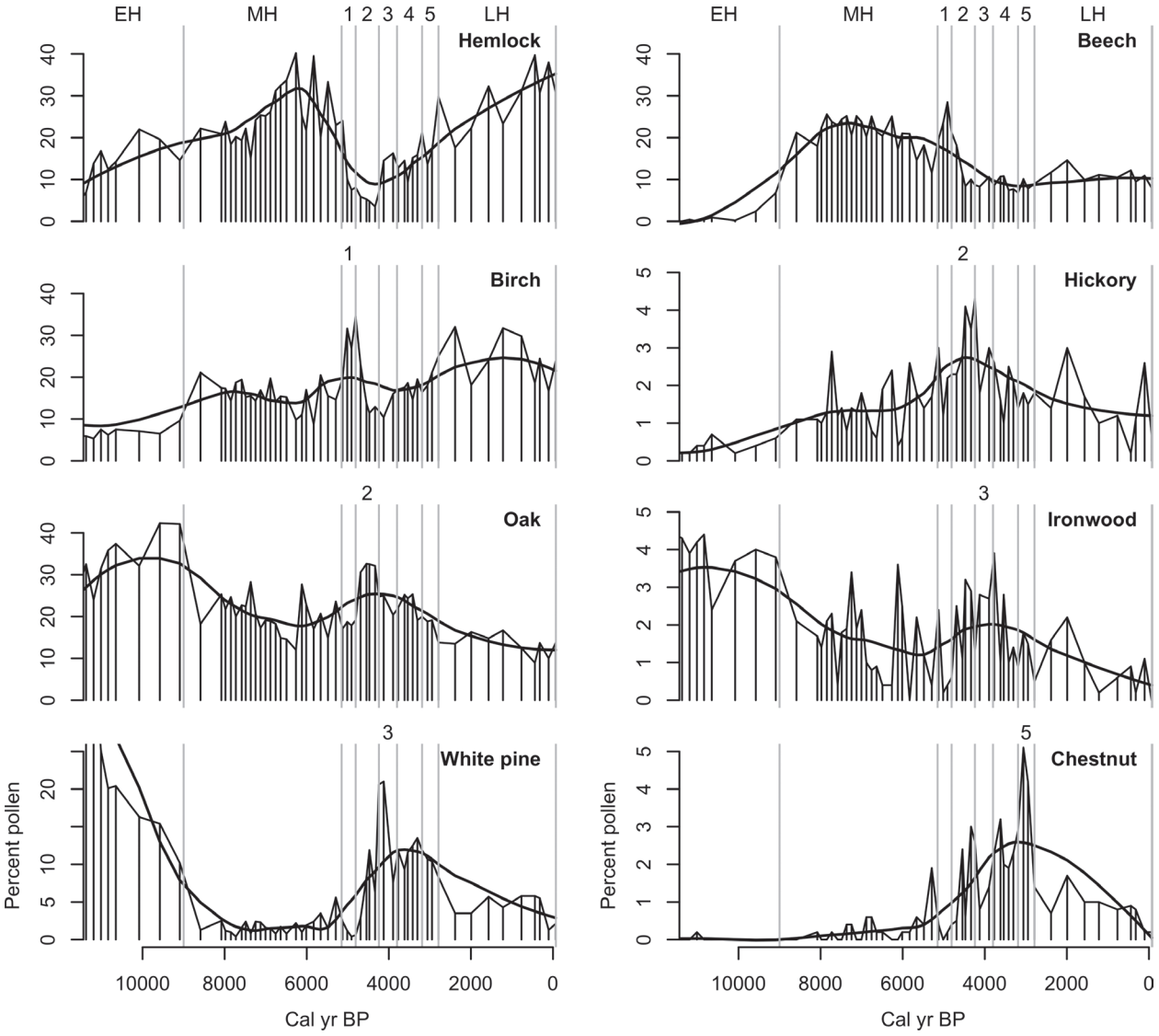

Figure 6. Sunfish Pond pollen percentages plotted by time. Loess smoothers (thick black lines) were fitted with 5000-yr spans. Vertical grey lines mark 11700, 9000, 5150, 4810, 4240, 3800, 3190 and 2790 YBP and divide the early Holocene (EH), mid Holocene before the hemlock decline (MH), the late Holocene (LH) and the five phases containing different peaks in pollen percentages of important tree taxa.

0.56 depending on the brGDGT calibration). Vegetation lags can be calculated as differences between pollen-inferred and independent (brGDGT) estimates of Holocene temperatures (Blonder et al. 2017; Shuman et al. 2019), but few significant differences exist between the two reconstructions (none since > 7000 YBP; Fig. 7B). The median difference of 0.04 °C (-0.71 - 0.92 °C, 95% C.I.) reveals no detectable lags, although one outlier brGDGT sample from 1174 YBP yields a temperature anomaly below -3.5 °C (> 4 standard deviations from the Holocene mean) and has been omitted here.

The brGDGTs indicate: 1) substantial warming before 10,000 YBP associated with increases in oak at Blanding and hemlock at Sunfish; 2) a transition between millennial-scale cool and warm phases at 5150-4880 YBP as hemlock declined; and 3) cooling after 2100 YBP as birch increased. The specific details depend upon the brGDGT calibration and some extreme variations with inconsistent calibrations may relate to non-temperature effects (Harning et al. 2025; Raberg et al. 2025), but the temperature changes also track those in the western North Atlantic Ocean (Shuman and Stefanescu 2025) and in other regional palaeotemperature indicators, including oxygen isotope ratios from Indiana (orange line, top row, Fig. 7A) (Gibson et al. 2024).

Locally, brGDGTs indicate that hemlock declined when mean temperatures above freezing (MAF) rose by ~ 1.1 °C (0.9–1.3 °C depending on the calibration) between 5150 (5300-5090) and 4880 (4890-4870) YBP; the same samples record the warming and the decline (black circles in Fig. 7B). The warming is also consistent with the hemlock decline where it has been closely dated elsewhere at 5025 (5160-4895 YBP; Booth et al. (2012)). The post-decline phase of peak birch and beech at Sunfish (phase 1, Fig. 6) preceded the subsequent maximum temperatures after 4880 YBP, which corresponded instead with high oak pollen percentages from ca. 4800-4200 YBP (phase 2 in Fig. 6). White pine peaked later as moisture increased, but then

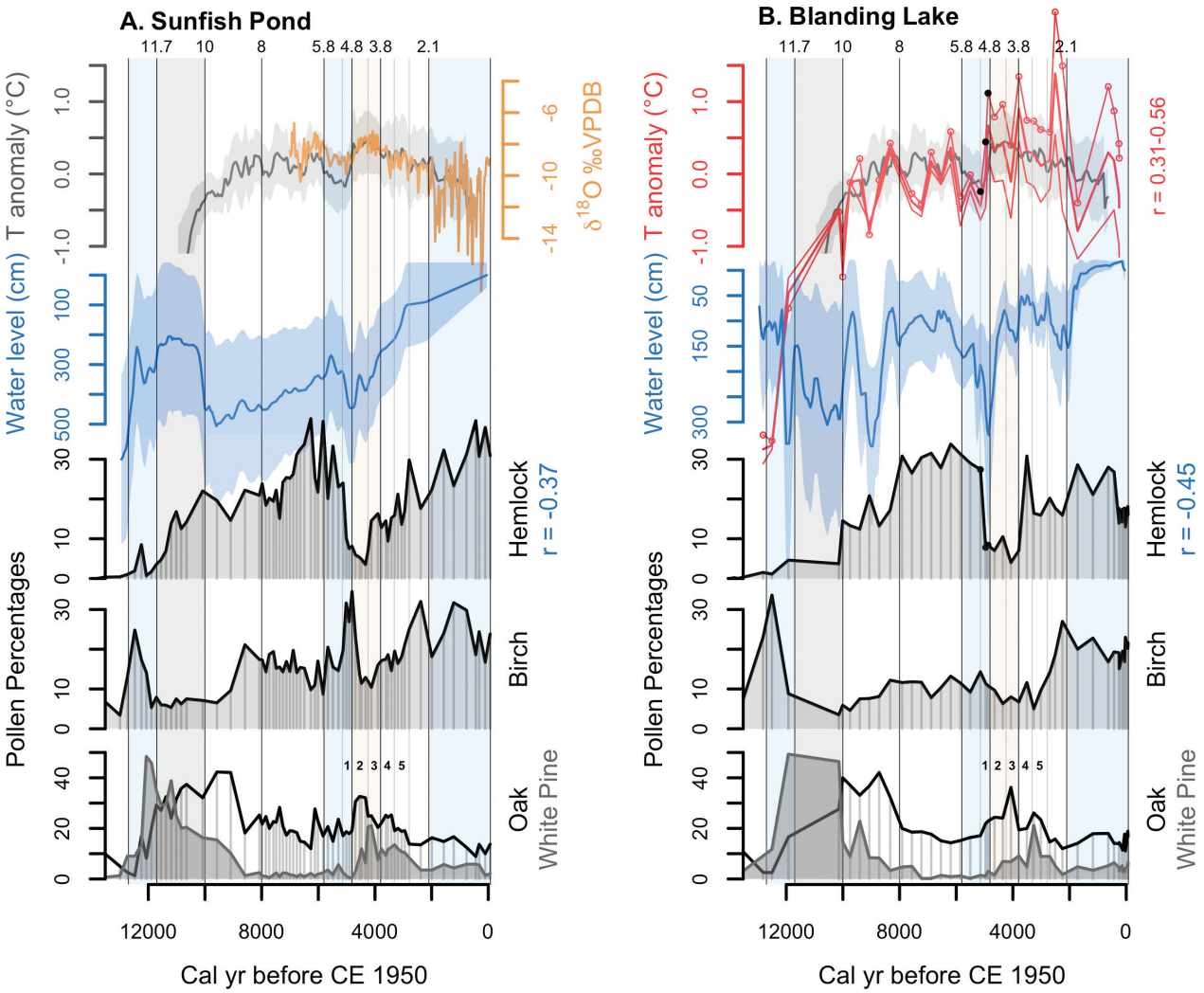

Figure 7. Comparison of pollen, temperature and lake-level reconstructions from: A) Sunfish Pond and B) Blanding Lake. The pollen percentages shown include hemlock (*Tsuga*), birch (*Betula*), oak (*Quercus*, unshaded) and white pine (*P. strobus*, grey line). Grey lines and uncertainty bands (top row) show pollen-inferred temperature (T) anomalies from the Holocene mean, averaged across mid-latitude sites from Iowa to Massachusetts (Shuman 2024); the overlying orange line in A shows the temperature-sensitive oxygen isotope record from Martin Lake, Indiana (Gibson et al. 2024). Branched GDGTs from Blanding Lake are calibrated to T anomalies using the global MBT'5me calibration (thin red line in B; Martínez-Sosa et al. (2021)) and 'meth set' calibration (red line with circles in B; Raberg et al. (2021)); thick red line shows the mean of the two calibrations. Black circles in B mark the brGDGT samples associated with the hemlock decline. Lake-level reconstructions (blue lines with 95% confidence intervals shaded) for each lake show their past levels below modern, based on palaeo-shoreline deposits in multiple near-shore cores, updated here to include data from the lake-centre core (in Fig. 2) from Blanding (Shuman and Burrell 2017; Ray-Cozzens 2022). Vertical lines, labelled by age in thousands of years, mark major temperature phases; thin grey lines also mark the century-scale vegetation phases in the mid-Holocene numbered as in Fig. 6.

both oak and pine declined as temperatures decreased by ca. 2100 YBP; > 20% birch pollen consistently coincided with low temperatures (vertical blue bars, Fig. 7).

Discussion

The forest changes recorded at the two lakes include multiple timescales of variation (Figs 4, 5) like those generated by our heuristic simulations of forest responses to Holocene climate changes (Fig. 2). The two records include the classic sequence of long-term vegetation trends and pollen zones consistent with the slowly varying aspects of the regional climate (Deevey 1943; Davis 1969; Watts 1979; Shuman et al. 2004) (Figs 4, 5). However, they also include additional millennial fluctuations (Fig. 6, smooth lines), superimposed centennial maxima and abrupt declines and increases (Fig. 6, raw data). Blanding Lake is representative of many records in the region with poorly resolved hints of the centennial variations. At Sunfish Pond, however, ~ 100-yr sample spacing clarifies the variability and reveals a sequence of events like that at other north-eastern highland and Tension Zone sites, such as Guilder and Little ponds, Massachusetts (Oswald et al. 2018) and Balsam and Ballston Lakes, New York (Ibe 1985; Toney et al. 2003) (Fig. 8).

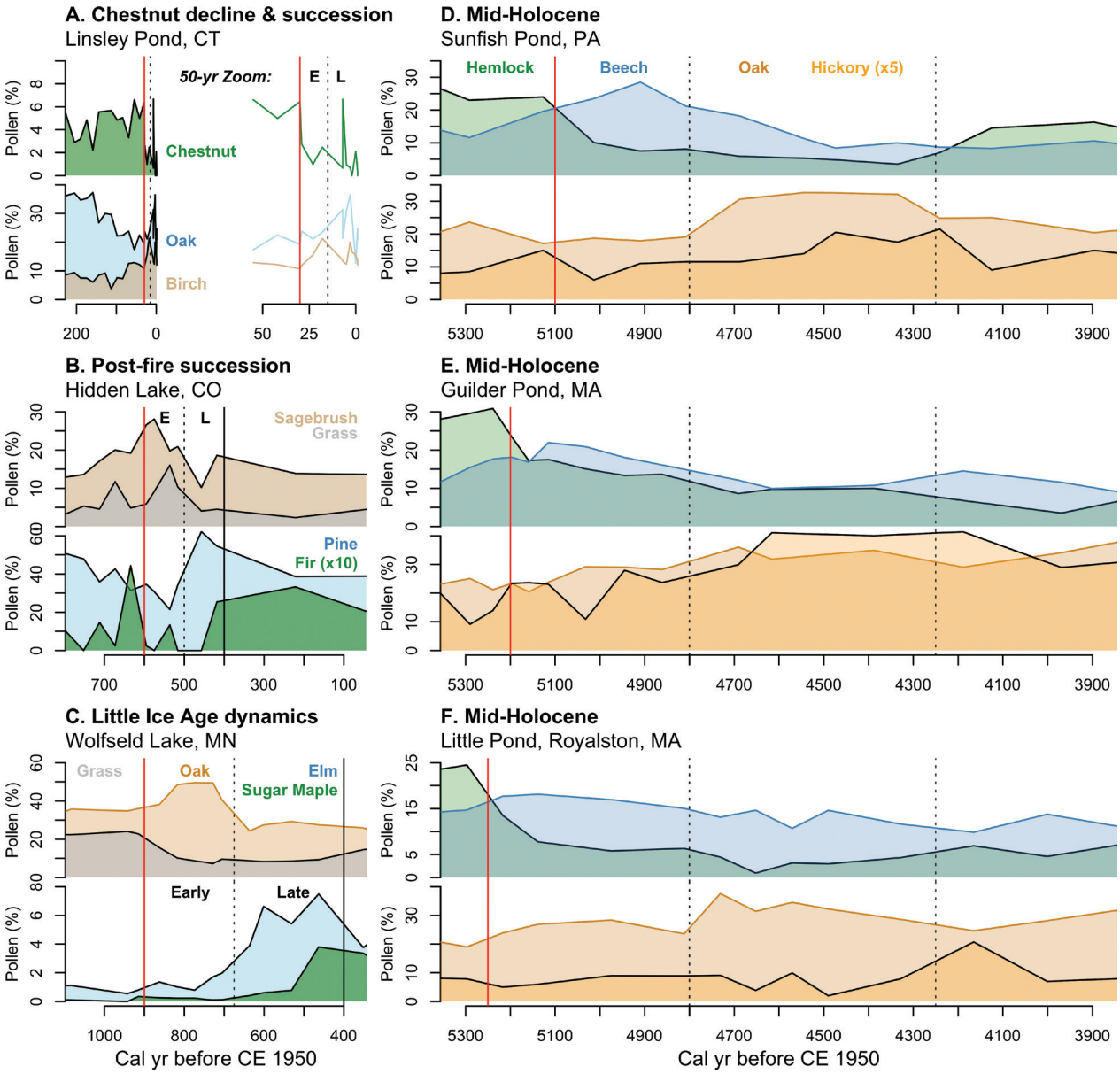

Figure 8. Fossil pollen records of known examples of successional dynamics (**A–C**) compared to mid-Holocene changes at (**D**) Sunfish Pond, PA and (**E, F**) comparator 'Tension Zone' lakes (Guilder and Little ponds, MA) (Oswald et al. 2018). Red vertical lines show the timing of disturbances or the first change in the series shown. Dashed lines mark the onset of subsequent vegetation phases, which are labelled as representing early ("E") or late ("L") successional phases in **A–C**. Unfilled line graphs in A zoom in on the details of the last 50 years there. All other timescales are the same showing 600 years in **A–C** and 1400 years in **D–F**.

Drivers of centennial-scale forest phases

A strong local correspondence amongst extreme drought, rapid warming and the abrupt hemlock decline points to climate variation as a driver of mid-Holocene forest turnover (Fig. 7). Likewise, the correlation of pollen-inferred temperatures with both the brGDGTs (Fig. 7B) and other temperature indicators (Fig. 7A) indicates a dynamic equilibrium between the forests and climate. The inference agrees with a large-scale analysis of climate and vegetation variability showing dynamic similarity at timescales of > 149 years (Fastovich et al. 2025). Based on an 'e-folding' time of ~ 75 years for succession in Appalachian forests, mid-Holocene forest phases lasting 340–610 years (Fig. 6) represent between 98.9 and 99.9% of the full equilibrium response; 95% would develop within ~ 225 years (per Equation 2; Webb III (1986)). Centennial-scale pollen sampling (Fig. 6) thus approximates the Nyquist frequency of near-equilibrium outcomes.

Comparing the centennial forest phases in Pennsylvania with other forest changes further clarifies the relevance of the dynamic equilibrium-niche model to the temporal and spatial scales of the mid-Holocene phases. Several alternative intrinsic forest dynamics, which we consider in turn below, do not appear to fit well with the observations: 1) competitive release and resulting successional dynamics following the hemlock

decline (Fuller 1998); 2) state-shifts triggered by repeated (compounded) disturbances (Turner et al. 1993; Paine et al. 1998); or 3) population variations shaped by the contingency of extreme events and autoregressive population processes (Jackson et al. 2009; Blaauw et al. 2010; Ramiadantsoa et al. 2019).

Competitive release and succession

Hemlock's removal from the forest could have released other taxa from competition for habitat and canopy space. For example, beech is an excellent gap-coloniser (Canham 1990; Poage and Peart 1993) and is often co-dominant with hemlock at the landscape scale (Fig. 1) (Cogbill et al. 2002). Consequently, beech could have had both an immediate and long-term competitive advantage after the hemlock decline (Fuller 1998). However, the various mid-Holocene mixtures of taxa do not wholly depend upon the decline and recovery of hemlock (Figs 4, 5). For example, white pine and chestnut became important for a millennium in the mid-Holocene at Blanding and Sunfish, but did not rapidly increase until after hemlock began its recovery (Fig. 6). At other sites across the Tension Zone region, increases in taxa like oak and pine sometimes began before the hemlock decline (Mott and Farley-Gill 1978) or even developed in the absence of abundant hemlock (Gilliam et al. 1967; Tzedakis 1992).

Three examples of succession recorded by other North American pollen records demonstrate responses to disturbance at landscape and larger scales (Fig. 8). However, these examples show unidirectional trajectories of seral stages over 25–250 years (Fig. 8), which differ in duration and progression from the repeated peaks and declines of the taxa near the Tension Zone (Fig. 6):

1. Succession following the removal of a single canopy species (Fig. 8A) - At Linsley Pond, Connecticut, the early-20th century chestnut blight caused a sharp decline in chestnut pollen percentages (red line, Fig. 8A) (Brugam 1978); Davis (1981) cited the example of the blight in making the case that the hemlock decline may have been driven by a similar disease. However, within 15 years of the blight, birch pollen percentages peaked, representing the early successional response ("E" in the 50-yr zoomed-in diagram, Fig. 8A). Within 30 years, oak pollen percentages had risen to replace both birch and chestnut during the late ("L") successional response. The sequence demonstrates that the successional responses to the rapid removal of a single key taxon would have played out far more rapidly than could be detected in the Sunfish Pond data and would not suitably explain centennial vegetation phases (Fig. 8D–F).
2. Succession following high-severity, stand-replacing fire (Fig. 8B) - At Hidden Lake, Colorado, pollen percentages illustrate the timescale of succession following high severity disturbance that removed much of a forest canopy (Calder et al. 2019). A large charcoal layer indicates a wildfire or series of fires at ca. 600 YBP (red line, Fig. 8B). After the fire, pollen percentages of trees declined and shrub or herbaceous taxa, such as sagebrush (*Artemisia*) and grass (Poaceae), increased to > 50% ("E" in Fig. 8B), which is unusual for a forested setting, but consistent with a post-fire meadow. After ~ 100 years, pine pollen percentages began increasing again, revealing post-fire lodgepole pine recovery, but by ~ 200 years after the fire, pine pollen percentages had peaked and declined as shade-tolerant, late-successional taxa, such as fir (*Abies*), increased ("L" in Fig. 8B). The 200-yr progression of phases involves the complete re-establishment of forest over a sufficiently large fraction of the pollen source area to be detectable here. However, the full progression is shorter than the 340–610-year duration of individual phases, such as the first beech-birch peak, at the Tension Zone sites (Fig. 8D–F).
3. Open woodland to deciduous forest transition during the Little Ice Age (Fig. 8C) - In the Big Woods region of Minnesota, climate changes and a regional reduction in wildfire favoured a transition from open oak woodlands to temperate deciduous forest (Grimm 1983; Umbanhowar 2004). Forest landscape simulations confirm that successional dynamics, including significant seed dispersal required to spread new trees across a large landscape, could explain the resulting sequence of changes (Berland et al. 2011). At first, the changes favoured an increase in oak, replacing grass and other herbaceous taxa (the "Early" phase in Fig. 8C). Then, shade-tolerant taxa, such as elm and sugar maple, increased at the expense of oak (the "Late" phase in Fig. 8C). The changes were likely asynchronous across the pollen source area, which caused the successional trends to persist longer than within individual stands (e.g. Bormann and Likens (1994)) or than after widely synchronised disturbances (Fig. 8A, B). The climate change may have extended the duration of each phase to 200–300 years (Fig. 8C). Simulations indicate, however, that such a climatic effect is not required; the duration is largely successional (Berland et al. 2011). Asynchronous stand-scale succession over large portions of a landscape can produce a slow, centennial-scale (but not multi-millennial) progression of taxa (Davis and Botkin 1985; Campbell and McAndrews 1993; Berland et al. 2011). If so, the e-folding time of succession at landscape scales may be 100–150, not 75 years.

However, unlike these examples, the tree sequences after the hemlock decline do not represent any obvious seral pattern or single progressive trajectory. Hemlock itself had brief periods of abundance and then secondary declines consistent with local changes in effective moisture (at 3510 YBP at Blanding Lake and 4250-3800 YBP at Sunfish Pond; Fig. 7) rather than a progressive return to a pre-disturbance state. Instead, if 95% of forest-climate equilibrium developed

within ~ 225 years, then the forest phases after the hemlock decline (Fig. 8D–F) would likely represent communities that grew as a function of different climates. Even a doubling of the e-folding time to 150 years would mean that the forest phases represented between 89.6 and 98.2% of equilibrium and a tripling to 225 years would mean 77.9–93.3%.

Compound disturbances, contingency effects and random walks

State shifts in forest composition can also emerge after multiple, repeated ("compound") disturbances with some species surviving an initial disturbance only to be killed by a second disturbance (Turner et al. 2019). Historical contingencies, i.e. the sequence of events, could influence how species respond to subsequent changes (Jackson et al. 2009). Stochastic population processes alone may also produce abrupt declines in the abundance of major tree taxa (Blaauw et al. 2010; Ramiadantsoa et al. 2019). However, the effects of disturbance and contingencies, if not population dynamics, would be highly localised because disturbances like storms, wildfires and drought tend to have small or heterogeneous spatial extents (e.g. Turner et al. (1998); Pederson et al. (2014)). Even the impacts of extremely large wildfire events appear as secondary features superimposed on close climate-pollen relationships in other settings (Calder and Shuman 2017). They are more likely to impact individual forest stands than whole regions. By contrast, the initial rise and then decline of beech, oak, hickory and pine played out similarly at multiple sites in different highland areas (Fig. 8D–F), which are unlikely to have been impacted by the same extreme events or population dynamics. Seed dispersal distances for the taxa here commonly reach 10s to 100s of metres with < 5% of seeds reaching > 1500-5000 m (He and Mladenoff 1999), which limits the connectivity amongst similar forest changes around Blanding and Sunfish (86 km apart), in western Massachusetts (Fig. 8E, F; ~ 300-400 km away) and at other Tension Zone sites in New York (~ 100-200 km away; Ibe (1985); Toney et al. (2003)) and Ontario (~ 300-400 km away; Bennett (1986); Fuller (1998)). All these locations lie well beyond the pollen source areas for our lakes, which should have radii of 3-14 km (Prentice 1988; Sugita 1993). Any ecological processes related to the decreases in beech and increases in oak spanning these distances along the Tension Zone would also have to predict well-correlated inverse patterns of change (beech increase and oak decrease) in coastal areas (Foster et al. 2006). Random walks cannot easily explain such patterning, but shifts in regional climate gradients can (Marsicek et al. 2013; Shuman et al. 2023).

Implications of the simulations for the hemlock decline and other abrupt changes

Our simulations demonstrate that sequences of abrupt tree declines at sites like Sunfish Pond (Fig. 6) do not necessarily require disturbances as triggers and that stochastic short-term climate variability could create differences amongst site-level details (Fig. 2). Fine-scale differences in the timing of detectable palaeoclimate and ecological changes are also not diagnostic of the processes involved; population processes, non-climatic disturbances and high-frequency climate variability could all accelerate ecological change compared to long-term climate trends. For example, the hemlock decline corresponded with rapid warming recorded by brGDGTs at Blanding Pond (Fig. 7B), but the decline cannot be assumed to be synchronous in detail across sites (Fig. 8D–F). Elsewhere, at Irwin Smith Bog, Michigan, hemlock declined at 5025 (5160–4895) YBP probably before it did at near-by Tower Lake at 4887 (5270–4855) YBP and almost certainly before drought lowered bog water levels there at 4858 (4951–4590) YBP (Booth et al. 2012). The fine-scale timing differences seem inevitable given any local, short-lived variability in hemlock abundance, such as the repeated, transient declines documented at Irwin Smith Bog (Booth et al. 2012) and other sites (e.g. Zhao et al. (2010); Oswald and Foster (2012)). As in the simulations, a site-specific population collapse, triggered by a range of causes, could have preceded the long-term drought and locally shifted the relative timing of events (Fig. 2E, F).

At ca. 5000 YBP, the truly unusual characteristic of the classic hemlock decline was the subsequent millennium of widespread low abundance (Fig. 7), not the decline's abruptness, which also applied to earlier and later events in Pennsylvania (Fig. 6) and elsewhere (Zhao et al. 2010; Booth et al. 2012; Oswald and Foster 2012). Davis (1981) initially ruled out climate as a driver of the hemlock decline and the low abundance that followed because evidence did not exist for substantial mid-Holocene climate changes, but that is no longer the case (Fig. 7) (see also Willard et al. (2005); Li et al. (2007); Menking et al. (2012); Shuman and Burrell (2017); Shuman et al. (2023); Shuman and Stefanescu (2025)). Like the low frequency aspects of pseudo-species' declines in our simulations (Fig. 2A), hemlock's prolonged mid-Holocene nadir overlaps in time with a unique climate that widely lowered water levels (Fig. 7; e.g. Shuman et al. (2004); Booth et al. (2012); Marsicek et al. (2013)) and raised temperatures at Blanding Lake (even as the underlying climate dynamics cooled northern areas; Shuman et al. (2023); Shuman (2024); Shuman (2025)). Our simulations show, however, that deterministic niche-based responses to the millennial climate trends would not preclude century-scale differences in the timing of events (Fig. 2E, F).

The model also reveals how differences in the climate niches (Fig. 2A–C) can create asynchrony in the declines of multiple taxa even when they represent responses to the same millennial or centennial climate oscillation (Fig. 2D). For example, the peaks and rapid declines of birch and beech, which followed the hemlock decline by ~ 300 years at Sunfish Pond (Figs 4, 5), represent a dynamic like the simulated sequence of declines in pseudo-species A (green) and then B (tan) several centuries later (Fig. 2F). The observed declines also correlate with the transition from a cold-dry to warm-dry mid-Holocene climate

(phases 1–2 in Fig. 7) in a manner consistent with their modern climate niches (Fig. 9) and the negative relationship between temperature and the longevity of trees like beech (Di Filippo et al. 2015).

Similar climate niches in space and time

As in the simulations, the different climate niches of the taxa at Blanding and Sunfish help to explain the forest histories (Fig. 9). Even though factors like land use have altered tree abundances today, the modern spatial realisation of the niches underlies the apparent accuracy of the pollen-inferred climate reconstructions examined here (grey lines, Fig. 7; Shuman et al. (2023); Shuman (2024)) and elsewhere (Lotter et al. 2000; Shuman et al. 2019). Space-for-time assumptions may not apply to locally-adapted traits like plant growth rates (Perret et al. 2024), but the correlations here suggest that climate-driven effects on life-history stages (e.g. recruitment), populations (e.g. demographic change) or genotypes (e.g. dispersal, selection), i.e. processes that enabled range-wide species-climate relationships to form today, converged on similar forest outcomes in the mid-Holocene (Davis and Shaw 2001; Blois et al. 2013) (Fig. 9).

For example, by 4800 YBP, the regional climate shifted to a warmer and drier climate than today (upper left shaded area in each panel of Fig. 9). The niches represented by modern pollen-climate relationships indicate that hemlock, but not beech and birch, could have declined as summer

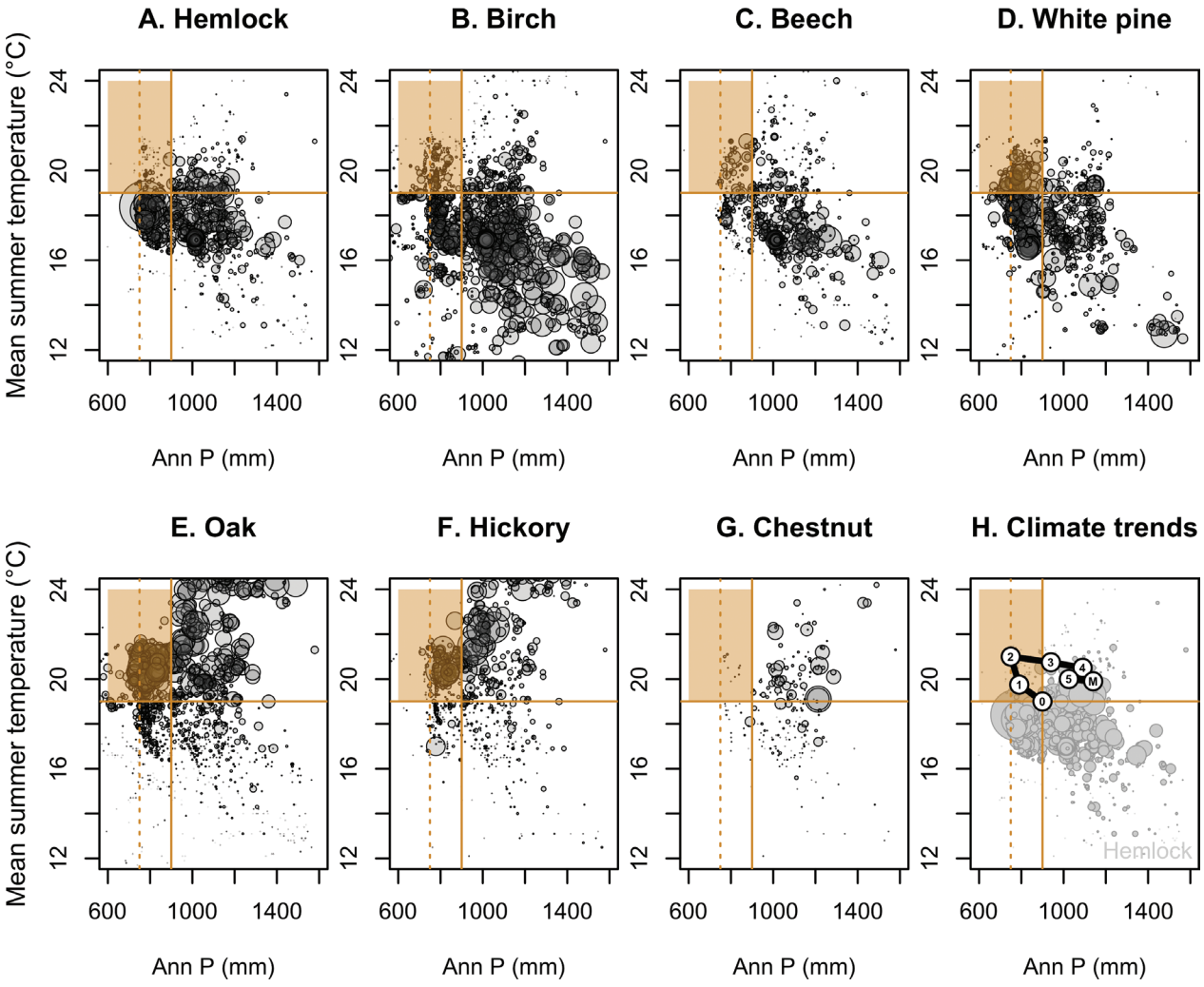

Figure 9. Modern pollen-climate relationships from North America east of 100°W longitude and north of 35°N latitude (Whitmore et al. 2005; Williams et al. 2006). Points show the relative abundances of hemlock (**A**), birch (**B**), beech (**C**), white pine (**D**), oak (**E**), hickory (**F**) and chestnut (**G**) pollen with respect to mean summer (June-August) temperatures and mean annual precipitation ("Ann P"). Climate trends informed by the GDGT and lake-level departures from modern (**H**) link the period before the hemlock decline (0) with each of the post-decline vegetation phases (1-5 in Figs 6, 7) and modern ("M"); the trends include millennial warmth combined with long-term moistening and centennial droughts (Fig. 7). Orange lines mark mean summer temperatures of 19 °C (horizontal solid line) and annual precipitation equal to 900 mm (vertical solid line) and 750 mm (vertical dashed line); orange shading marks wetter and warmer climates than the solid line thresholds where hemlock is absent, but not other taxa like beech. Circle sizes are scaled to abundance in each sample; oak and birch symbols are scaled to one-third the size of hemlock, beech and white pine and one-sixth the size of hickory and chestnut to account for differences in total abundance.

temperatures increased and precipitation fell (phase 1 in the upper left quadrants, shading, Fig. 9); hemlock is rare today and throughout the Holocene in the parts of southern Michigan, Ohio and western New York represented by this warm, dry part of the niche space (Prentice et al. 1991; Thompson et al. 1999; Williams et al. 2006). Later climate changes further warmed and dried the climate (phase 2, Fig. 9), favouring oak and hickory over beech, which would have then declined. As the region ultimately cooled and moistened towards the present (phases 3–5, Fig. 9), other taxa like white pine (Fig. 9D) and chestnut (Fig. 9G) would have increased before substantial cooling favoured taxa like birch and hemlock again since 2100 YBP (Fig. 7).

Changes in the Tension Zone

The interaction amongst climate changes and different niches has a spatial analogy in 18th century forests (Fig. 1) (Cogbill et al. 2002; Thompson et al. 2013). Walther's Law states that stratigraphically adjacent palaeoenvironments typically have equivalents in spatially-adjacent environments today (Middleton 1973). It applies well to the sequences of mid-Holocene forest phases at Blanding and Sunfish. Cold-hardy, mesic hemlock-beech-birch forests grew north of the Tension Zone ecotone at the time of European colonisation (green, yellow, Fig. 1). To the south, a narrow band of white pine forests helped to define the 18th century ecotone (blue, Fig. 1); oak-dominated forests extended southwards from there (tan, Fig. 1). After the rapid mid-Holocene warming by ca. 4800 YBP (Fig. 7), the Tension Zone passed northwards as oak populations expanded and replaced hardwood and conifer stands around Sunfish and Blanding. Oak abundance locally became equivalent to southern sites, such as Tannersville Swamp (Fig. 1) (Watts 1979). With cooling after ca. 3800 YBP, the ecotone again shifted southwards: the pine belt (grey shading, bottom row, Fig. 7) and then renewed hardwoods replaced the mid-Holocene oak forests (e.g. hemlock and birch in Fig. 7).

The Holocene moistening trend that raised the lake levels (Fig. 7) (Shuman et al. 2019) further modified the spatial patterns of vegetation change. The long-term increase in effective moisture created a general westward shift in ecoclimatic conditions; after ca. 4500 YBP, the region with < 1000 mm of annual precipitation shifted westwards out of Pennsylvania into the Ohio River Valley and surrounding regions where such conditions exist today. Both low-hemlock phases at Sunfish, i.e. the beech-dominated phase during cool conditions from 5000–4800 YBP and the subsequent oak-hickory peak associated with high temperatures from 4800–4250 YBP, have similarities to historic forests in the dry climates of western New York, Ohio, Indiana and Michigan (Fig. 1) (Paciorek et al. 2016). As moisture increased, such forests shifted westwards. In other words, the Tension Zone shifted northwards during the oak-dominated warm phase from 4800–4250 YBP (Phase 2 in Fig. 7), but a beech-birch phase (phase 1 in Fig. 6) preceded the shift and pine-chestnut phases (3–5 in Fig. 6) followed after it because the temperature maximum and attendant ecotone oscillation developed amid a long-term increase in effective moisture that changed the ecotonal forest communities (Fig. 7).

Conclusions

Appalachian forests, such as those around Blanding Lake and Sunfish Pond, never achieved persistent steady states. Distinct forest communities repeatedly developed and then dissipated within 300–500 years. Some (e.g. oak-dominated phases) formed and reformed, but others (e.g. the beech-birch phase at Sunfish Pond) formed only once. The landscape-scale changes and the extensive communities that they produced did not appear to represent successional sequences (Fig. 8) or random-walk trajectories contingent on a "ratcheting" sequence of droughts or population dynamics (Paine et al. 1998; Jackson et al. 2009). These successional or stochastic processes should have produced poor correlations with climate history and differences across large geographic areas (Clark and McLachlan 2003); they also should have either similarities to known successional patterns or no predictable sequences, but neither expectation was met (Figs 7, 8). Instead, despite concerns that species' responses to spatial climate gradients would not predict their changes through time (Perret et al. 2024), pollen-inferred temperatures, based on a space-for-time assumption, agree with independent temperature proxies (e.g. top row, Fig. 7; see also Shuman et al. (2019) for a more quantitative analysis). Individual taxa, such as hemlock, birch and oak, also expressed relationships with the independent temperature (brGDGT) and moisture (lake-level) histories (Fig. 7) consistent with the realisation of the taxa's climate niches across space today (Fig. 9). The patterns of change in the forest histories (Fig. 6) do not differ meaningfully from the types of abrupt changes, fluctuations and short-lived phases generated by a simple deterministic response to a variable climate (Fig. 2) and indicate that the emergent outcomes over many forest stands converged on centennial scales on a dynamic equilibrium with climate (Webb III 1986; Shuman et al. 2019).

Small differences in species' climate relationships can explain the individualistic responses of the key tree taxa to the climate changes. Consequently, both climate history and the climate niches of the different taxa could be better studied, along with direct evidence of forest disturbances and plant physiological responses to shifting climates, to help explain the past and anticipate the future; for example, just because both hemlock and beech are 'mesic' taxa did not mean that they responded to mid-Holocene climatic variability in the same way (compare their presence in the orange shaded region of Fig. 9). The species declines, the resulting novel forest communities and shifts in the Tension Zone developed rapidly in concert with unique, centennial-to-millennial combinations of temperature and moisture (Figs 7, 9). Consequently, vegetation at landscape

scales appears highly sensitive to climate changes. If ~ 1 °C of warming triggered the hemlock decline, warming will yield complex, rapid forest changes again today.

Acknowledgements

We thank J. Williams and A. Seddon for constructive reviews, D. Foster and W. Oswald for additional useful comments on the manuscript and A. Perrotti for processing pollen samples. We also thank J. Rodysill and J. Donnelly for help identifying Sunfish Pond as a study site and students in the 2015 summer research experience programme of the Roy J. Shlemon Center for Quaternary Studies for help collecting the Blanding Lake and Sunfish Pond cores. Funding was provided by the Roy J. Shlemon Center for Quaternary Studies at the University of Wyoming and NSF Division of Environmental Biology (DEB-1856047; DEB-1855822).

Author contributions statement

BNS conceived the study. IS, ICS and TRC collected data. BNS carried out statistical analyses. BNS wrote the first manuscript version. BNS, IS, JJ and DMN commented and made edits to the manuscript. All authors gave permission for its publication.

Use of AI

No use of AI was reported.

Data accessibility statement

Pollen data are available through the Neotoma Paleoecology Database (https://www.neotomadb.org/) and the palaeoclimate reconstructions through the NOAA Palaeoclimatology data centre (https://www.ncei.noaa.gov/products/paleoclimatology).

References

Allison TD, Moeller RE, Davis MB (1986) Pollen in laminated sediments provides evidence for a mid-Holocene forest pathogen outbreak. Ecology 67: 1101–1105. https://doi.org/10.2307/1939835

Anderson RS, Davis RB, Miller NG, Stuckenrath R (1986) History of late- and post-glacial vegetation and disturbance around Upper South Branch Pond, northern Maine. Canadian Journal of Botany 64: 1977–1986. https://doi.org/10.1139/b86-262

Baker WL (1989) Landscape ecology and nature reserve design in the Boundary Waters Canoe Area, Minnesota. Ecology 70: 23–35. https://doi.org/10.2307/1938409

Barnosky AD, Barnosky CW, Nickmann RJ, Ashworth AC, Schwert DP, Lantz SW (1988) Late Quaternary paleoecology at the Newton Site, Bradford Co., northeastern Pennsylvania: *Mammuthus columbi*, palynology, and fossil insects. Bulletin of the Buffalo Society of Natural Sciences 33: 173–184.

Bennett KD (1986) Holocene history of forest trees in southern Ontario. Canadian Journal of Botany 65: 1792–1801. https://doi.org/10.1139/b87-248

Berg TM, Edmunds WE, Geyer AR (1980) Geologic map of Pennsylvania. Second Edition, scale 1:250,000.

Berland A, Shuman B, Manson S (2011) Simulated importance of dispersal, disturbance, and landscape history in long-term ecosystem change in the Big Woods of Minnesota. Ecosystems 14: 398–414. https://doi.org/10.1007/s10021-011-9418-x

Bernabo JC, Webb III T (1977) Changing patterns in the Holocene pollen record from northeastern North America: a mapped summary. Quaternary Research 8: 64–96. https://doi.org/10.1016/0033-5894(77)90057-6

Bhiry N, Filion L (1996) Mid-Holocene hemlock decline in eastern North America linked with phytophagous insect activity. Quaternary Research 45: 312. https://doi.org/10.1006/qres.1996.0032

Blaauw M, Bennett KD, Christen JA (2010) Random walk simulations of fossil proxy data. The Holocene 20: 645–649. https://doi.org/10.1177/0959683609355180

Blois JL, Williams JW, Fitzpatrick MC, Jackson ST, Ferrier S (2013) Space can substitute for time in predicting climate-change effects on biodiversity. Proceedings of the National Academy of Sciences 110: 9374–9379. https://doi.org/10.1073/pnas.1220228110

Blonder B, Moulton DE, Blois J, Enquist BJ, Graae BJ, Macias Fauria M, McGill B, Nogué S, Ordonez A, Sandel B, Svenning JC (2017) Predictability in community dynamics. Ecology Letters 20: 293–306. https://doi.org/10.1111/ele.12736

Booth RK, Brewer S, Blaauw M, Minckley TA, Jackson ST (2012) Decomposing the mid-Holocene *Tsuga* decline in eastern North America. Ecology 93: 1841–1852. https://doi.org/10.1890/11-2062.1

Bormann FH, Likens GE (1994) Pattern and process in a forested ecosystem: disturbance, development, and the steady state based on the Hubbard Brook ecosystem study. Springer-Verlag, New York. https://doi.org/10.1007/978-1-4612-6232-9_6

Bradbury JA, Keim BD, Wake CP (2003) The influence of regional storm tracking and teleconnections on winter precipitation in the northeastern United States. Annals of the Association of American Geographers 93: 544–556. https://doi.org/10.1111/1467-8306.9303002

Brady RH, Waldstreicher JS (2001) Observations of mountain wave–induced precipitation shadows over northeast Pennsylvania. Weather and Forecasting 16: 281–300. https://doi.org/10.1175/1520-0434(2001)016%3C0281:OOMWIP%3E2.0.CO;2

Braun DD (2004) The glaciation of Pennsylvania, USA. In: Ehlers J, Gibbard PL (Eds) Developments in Quaternary Sciences Vol. 2, Part B, Elsevier, Oxford, 237–242. https://doi.org/10.1016/S1571-0866(04)80201-X

Brugam RB (1978) Pollen indicators of land-use change in southern Connecticut. Quaternary Research 9: 349–362. https://doi.org/10.1016/0033-5894(78)90038-8

Calcote R (2003) Mid-Holocene climate and the hemlock decline: the range limit of *Tsuga* canadensis in the western Great Lakes region, USA. The Holocene 13: 215. https://doi.org/10.1191/0959683603hl608rp

Calder WJ, Shuman B (2017) Extensive wildfires, climate change, and an abrupt state change in subalpine ribbon forests, Colorado. Ecology 98: 2585–2600. https://doi.org/10.1002/ecy.1959

Calder WJ, Stefanova I, Shuman B (2019) Climate–fire–vegetation interactions and the rise of novel landscape patterns in subalpine ecosystems, Colorado. Journal of Ecology 107: 1689–1703. https://doi.org/10.1111/1365-2745.13138

Campbell ID, McAndrews JH (1993) Forest disequilibrium caused by rapid Little Ice Age cooling. Nature 366: 336–338. https://doi.org/10.1038/366336a0

Canham CD (1990) Suppression and release during canopy recruitment in *Fagus grandifolia*. Bulletin of the Torrey Botanical Club 117: 1–7. https://doi.org/10.2307/2997123

Chartrand J, Pausata FSR (2020) Impacts of the North Atlantic Oscillation on winter precipitations and storm track variability in southeast Canada and the northeast United States. Weather and Climate Dynamics 1: 731–744. https://doi.org/10.5194/wcd-1-731-2020

Clark JS, McLachlan JS (2003) Stability of forest biodiversity. Nature 423: 635–638. https://doi.org/10.1038/nature01632

Clifford MJ, Booth RK (2015) Late-Holocene drought and fire drove a widespread change in forest community composition in eastern North America. The Holocene 25: 1102–1110. https://doi.org/10.1177/0959683615580182

Cogbill CV, Burk J, Motzkin G (2002) The forests of presettlement New England, USA: spatial and compositional patterns based on town proprietor surveys. Journal of Biogeography 29: 1279–1304. https://doi.org/10.1046/j.1365-2699.2002.00757.x

Davis MB (1969) Climatic changes in southern Connecticut recorded by pollen deposition at Rogers Lake. Ecology 50: 409–422. https://doi.org/10.2307/1933891

Davis MB (1981) Outbreaks of forest pathogens in Quaternary history. Proceedings of the Fourth International Palynological Conference 3: 216–227.

Davis MB, Botkin D (1985) Sensitivity of cool-temperate forests and their fossil pollen record to rapid temperature change. Quaternary Research 23: 327–340. https://doi.org/10.1016/0033-5894(85)90039-0

Davis MB, Shaw RG (2001) Range shifts and adaptive responses to Quaternary climate change. Science 292: 673–679. https://doi.org/10.1126/science.292.5517.673

De Jonge C, Peterse F, Nierop KGJ, Blattmann TM, Alexandre M, Ansanay Alex S, Austin T, Babin M, Bard E, Bauersachs T, Blewett J, Boehman B, Castañeda IS, Chen J, Conti MLG, Contreras S, Cordes J, Davtian N, van Dongen B, Duncan B, Elling FJ, Galy V, Gao S, Hefter J, Hinrichs K-U, Helling MR, Hoorweg M, Hopmans E, Hou J, Huang Y, Huguet A, Jia G, Karger C, Keely BJ, Kusch S, Li H, Liang J, Lipp JS, Liu W, Lu H, Mangelsdorf K, Manners H, Martinez Garcia A, Menot G, Mollenhauer G, Naafs BAD, Naeher S, O'Connor LK, Pearce EM, Pearson A, Rao Z, Rodrigo-Gámiz M, Rosendahl C, Rostek F, Bao R, Sanyal P, Schubotz F, Scott W, Sen R, Sluijs A, Smittenberg R, Stefanescu I, Sun J, Sutton P, Tierney J, Tejos E, Villanueva J, Wang H, Werne J, Yamamoto M, Yang H, Zhou A (2024) Interlaboratory comparison of branched GDGT temperature and pH proxies using soils and lipid extracts. Geochemistry, Geophysics, Geosystems 25(7): e2024GC011583. https://doi.org/10.1029/2024GC011583

Deevey ES (1943) Additional pollen analyses from southern New England. American Journal of Science 241: 717–752. https://doi.org/10.2475/ajs.241.12.717

Di Filippo A, Pederson N, Baliva M, Brunetti M, Dinella A, Kitamura K, Knapp HD, Schirone B, Piovesan G (2015) The longevity of broadleaf deciduous trees in Northern Hemisphere temperate forests: insights from tree-ring series. Frontiers in Ecology and Evolution 3: 46. https://doi.org/10.3389/fevo.2015.00046

Fægri K, Iversen J, Kaland PE, Krzywinski K (1992) Textbook of Pollen Analysis. Fourth Edition. J. Wiley, Sons, Chichester.

Fastovich D, Meyers SR, Saupe EE, Williams JW, Dornelas M, Dowding EM, Finnegan S, Huang HHM, Jonkers L, Kiessling W, Kocsis ÁT (2025) Coupled, decoupled, and abrupt responses of vegetation to climate across timescales. Science 389: 64–68. https://doi.org/10.1126/science.adr6700

Foster DR, Boose ER (1992) Patterns of forest damage resulting from catastophic wind in central New England. The Journal of Ecology 80: 79. https://doi.org/10.2307/2261065

Foster DR, Clayden S, Orwig DA, Hall B, Barry S (2002) Oak, chestnut and fire: climatic and cultural controls of long-term forest dynamics in New England, USA. Journal of Biogeography 29: 1359–1379. https://doi.org/10.1046/j.1365-2699.2002.00760.x

Foster DR, Oswald WW, Faison EK, Doughty ED, Hansen BCS (2006) A climatic driver for abrupt mid-Holocene vegetation dynamics and the hemlock decline in New England. Ecology 87: 2959–2966. https://doi.org/10.1890/0012-9658(2006)87[2959:ACDFAM]2.0.CO;2

Fuller JL (1998) Ecological impact of the mid-Holocene hemlock decline in southern Ontario, Canada. Ecology 79: 2337–2351. https://doi.org/10.1890/0012-9658(1998)079[2337:EIOTMH]2.0.CO;2

Fuller TL, Foster DR, McLachlan TS, Drake N (1998) Impact of human activity on regional forest composition and dynamics in central New England. Ecosystems 1: 76–95. https://doi.org/10.1007/s100219900007

Gaudreau D, Webb III T (1985) Late-Quaternary pollen stratigraphy and isochrone maps for the northeastern United States. In: Bryant J, Halloway RG (Eds) Pollen records of Late-Quaternary North American sediments. American Association of Stratigraphic Palynologists, Dallas, 247–280.

Gibson DK, Bird BW, Finney BP, Steinman BA (2024) Holocene insolation and sea surface temperature influences on the polar front jet stream and precipitation in the midcontinental United States. Quaternary Science Reviews 340: 108865. https://doi.org/10.1016/j.quascirev.2024.108865

Gilliam JA, Kapp RO, Bogue RD (1967) A post-Wisconsin pollen sequence from Vestaburg Bog, Moncalm County, Michigan. Michigan Academy of Science, Arts and Letters 52: 3–17.

Grimm EC (1983) Chronology and dynamics of vegetation change in the prairie-woodland region of southern Minnesota, U.S.A. New Phytologist 93: 311–350. https://doi.org/10.1111/j.1469-8137.1983.tb03434.x

Grimm EC (1987) CONISS: a FORTRAN 77 program for stratigraphically constrained cluster analysis by the method of incremental sum of squares. Computers, Geosciences 13: 13–35. https://doi.org/10.1016/0098-3004(87)90022-7

Grubb PJ (1977) The maintenance of species-richness in plant communities: The importance of the regeneration niche. Biological Reviews 52: 107–145. https://doi.org/10.1111/j.1469-185X.1977.tb01347.x

Harning DJ, Sacco S, Raberg JH, Ardenghi N, Sepúlveda J, Shapiro B, Miller GH, Geirsdóttir Á (2025) Both redox potential and climate control molecular proxies in Icelandic Holocene lake sediments. Communications Earth, Environment 6: 763. https://doi.org/10.1038/s43247-025-02701-7

Haslett J, Parnell A (2008) A simple monotone process with application to radiocarbon-dated depth chronologies. Journal of the Royal Statistical Society: Series C (Applied Statistics) 57: 399–418. https://doi.org/10.1111/j.1467-9876.2008.00623.x

He HS, Mladenoff DJ (1999) Spatially explicit and stochastic simulations of forest-landscape fire disturbance and succession. Ecology 80: 81–99. https://doi.org/10.1890/0012-9658(1999)080[0081:SEASSO]2.0.CO;2

Hopmans EC, Schouten S, Sinninghe Damsté JS (2016) The effect of improved chromatography on GDGT-based palaeoproxies. Organic Geochemistry 93: 1–6. https://doi.org/10.1016/j.orggeochem.2015.12.006

Ibe RA (1985) Postglacial montane vegetational history around Balsam Lake, Catskill Mountains, New York. Bulletin of the Torrey Botanical Club 112: 176–186. https://doi.org/10.2307/2996414

Jackson ST, Betancourt JL, Booth RK, Gray ST (2009) Ecology and the ratchet of events: Climate variability, niche dimensions, and species distributions. Proceedings of the National Academy of Sciences of the United States of America 106: 19685–19692. https://doi.org/10.1073/pnas.0901644106

Jackson ST, Blois JL (2015) Community ecology in a changing environment: Perspectives from the Quaternary. Proceedings of the National Academy of Sciences 112: 4915–4921. https://doi.org/10.1073/pnas.1403664111

Juggins S (2024) rioja: analysis of Quaternary science data, R package version (1.0–7). https://cran.r-project.org/package=rioja

Li Y-X, Yu Z, Kodama KP (2007) Sensitive moisture response to Holocene millennial-scale climate variations in the Mid-Atlantic region, USA. The Holocene 17: 3–8. https://doi.org/10.1177/0959683606069386

Lotter AF, Birks HJB, Eicher U, Hofmann W, Schwander J, Wick L (2000) Younger *Dryas* and Allerød summer temperatures at Gerzensee (Switzerland) inferred from fossil pollen and cladoceran assemblages. Palaeogeography, Palaeoclimatology, Palaeoecology 159: 349–361. https://doi.org/10.1016/S0031-0182(00)00093-6

Maenza-Gmelch TE (1997) Holocene vegetation, climate, and fire history of the Hudson Highlands, southeastern New York, USA. The Holocene 7: 25–37. https://doi.org/10.1177/095968369700700103

Marsicek JP, Shuman B, Brewer S, Foster DR, Oswald WW (2013) Moisture and temperature changes associated with the mid-Holocene *Tsuga* decline in the northeastern United States. Quaternary Science Reviews 80: 333–342. https://doi.org/10.1016/j.quascirev.2013.09.001

Martínez-Sosa P, Tierney JE, Stefanescu IC, Dearing Crampton-Flood E, Shuman BN, Routson C (2021) A global Bayesian temperature calibration for lacustrine brGDGTs. Geochimica et Cosmochimica Acta 305: 87–105. https://doi.org/10.1016/j.gca.2021.04.038

Mayle FE, Levesque AJ, Cwynar LC (1993) *Alnus* as an indicator taxon of the Younger Dryas cooling in eastern North America. Quaternary Science Reviews 12: 295–305. https://doi.org/10.1016/0277-3791(93)90038-N

Menking KM, Peteet DM, Anderson RY (2012) Late-glacial and Holocene vegetation and climate variability, including major droughts, in the Sky Lakes region of southeastern New York State. Palaeogeography, Palaeoclimatology, Palaeoecology 353–355: 45–59. https://doi.org/10.1016/j.palaeo.2012.06.033

Middleton AD (1973) Johannes Walther's Law of the correlation of facies. GSA Bulletin 84: 979–988. https://doi.org/10.1130/0016-7606(1973)84%3C979:JWLOTC%3E2.0.CO;2

Mott RJ, Farley-Gill LD (1978) A Late-Quaternary pollen profile from Woodstock, Ontario. Canadian Journal of Earth Sciences 15: 1101–1111. https://doi.org/10.1139/e78-116

Myers RE (1954) The geology of Bradford County, Pennsylvania. Rocks, Minerals 29: 144–178. https://doi.org/10.1080/00357529.1954.11767008

Nowacki GJ, Abrams MD (2015) Is climate an important driver of post-European vegetation change in the Eastern United States? Global Change Biology 21: 314–334. https://doi.org/10.1111/gcb.12663

Nowacki GJ, Abrams MD (2008) The demise of fire and "mesophication" of forests in the eastern United States. BioScience 58: 123–138. https://doi.org/10.1641/B580207

Oswald WW, Doughty ED, Foster DR, Shuman BN, Wagner DL (2016) Evaluating the role of insects in the middle-Holocene *Tsuga* decline. The Journal of the Torrey Botanical Society 144: 35–39. https://doi.org/10.3159/TORREY-D-15-00074.1

Oswald WW, Faison EK, Foster DR, Doughty ED, Hall BR, Hansen BCS (2007) Post-glacial changes in spatial patterns of vegetation across southern New England. Journal of Biogeography 34: 900–913. https://doi.org/10.1111/j.1365-2699.2006.01650.x

Oswald WW, Foster DR (2012) Middle-Holocene dynamics of *Tsuga canadensis* (eastern hemlock) in northern New England, USA. The Holocene 22: 71–78. https://doi.org/10.1177/0959683611409774

Oswald WW, Foster DR, Shuman BN, Chilton ES, Doucette DL, Duranleau DL (2020) Conservation implications of limited Native American impacts in pre-contact New England. Nature Sustainability 3: 241–246. https://doi.org/10.1038/s41893-019-0466-0

Oswald WW, Foster DR, Shuman BN, Doughty ED, Faison EK, Hall BR, Hansen BCS, Lindbladh M, Marroquin A, Truebe SA (2018) Subregional variability in the response of New England vegetation to postglacial climate change. Journal of Biogeography 45: 2375–2388. https://doi.org/10.1111/jbi.13407

Paciorek CJ, Goring SJ, Thurman AL, Cogbill CV, Williams JW, Mladenoff DJ, Peters JA, Zhu J, McLachlan JS (2016) Statistically-estimated tree composition for the northeastern United States at Euro-American settlement. PLOS ONE 12(1): e0150087. https://doi.org/10.1371/journal.pone.0150087

Paine RT, Tegner MJ, Johnson EA (1998) Compounded perturbations yield ecological surprises. Ecosystems 1: 535–545. https://doi.org/10.1007/s100219900049

Parnell AC, Haslett J, Allen JRM, Buck CE, Huntley B (2008) A flexible approach to assessing synchroneity of past events using Bayesian reconstructions of sedimentation history. Quaternary Science Reviews 27: 1872–1885. https://doi.org/10.1016/j.quascirev.2008.07.009

Pederson N, Dyer JM, McEwan RW, Hessl AE, Mock CJ, Orwig DA, Rieder HE, Cook BI (2014) The legacy of episodic climatic events in shaping temperate, broadleaf forests. Ecological Monographs 84: 599–620. https://doi.org/10.1890/13-1025.1

Perret DL, Evans MEK, Sax DF (2024) A species' response to spatial climatic variation does not predict its response to climate change. Proceedings of the National Academy of Sciences 121(1): e2304404120. https://doi.org/10.1073/pnas.2304404120

Peteet DM, Vogel JS, Nelson DE, Southon JR, Nickmann RJ, Heusser LE (1990) Younger *Dryas* climatic reversal in northeastern USA? AMS ages for an older problem. Quaternary Research 33: 219–230. https://doi.org/10.1016/0033-5894(90)90020-L

Peterson AT, Soberon J, Pearson RG, Anderson RP, Martinez-Meyer E, Nakamura M, Araújo MB (2011) Ecological Niches and Geographic Distributions. Princeton University Press, Princeton, N.J. https://doi.org/10.23943/princeton/9780691136868.003.0003

Poage NJ, Peart DR (1993) The radial growth response of American Beech (*Fagus grandifolia*) to small canopy gaps in a northern hardwood forest. Bulletin of the Torrey Botanical Club 120: 45–48. https://doi.org/10.2307/2996662

Prentice IC (1988) Records of vegetation in time and space: the principles of pollen analysis. In: Huntley B, Webb III T (Eds) Vegetation History. Handbook of Vegetation Science, Kluwer Academic Publishers, Dordrecht, 17–42. https://doi.org/10.1007/978-94-009-3081-0_2

Prentice IC, Bartlein PJ, Webb III T (1991) Vegetation and climate changes in eastern North America since the last glacial maximum: A response to continuous climatic forcing. Ecology 72: 2038–2056. https://doi.org/10.2307/1941558

PRISM Climate Group (2022) PRISM Climate Group. http://prism.oregonstate.edu [created December 2022]

R Core Development Team (2022) R: A language and environment for statistical computing. R Foundation for Statistical Computing, Vienna, Austria.

Raberg JH, Harning DJ, Crump SE, de Wet G, Blumm A, Kopf S, Geirsdóttir Á, Miller GH, Sepúlveda J (2021) Revised fractional abundances and warm-season temperatures substantially improve brGDGT calibrations in lake sediments. Biogeosciences 18: 3579–3603. https://doi.org/10.5194/bg-18-3579-2021

Raberg JH, de Wet GA, Geirsdóttir Á, Sepúlveda J, Miller GH (2025) Oxygen depletion in lake waters may skew brGDGT-inferred temperatures by more than 10 °C. Geophysical Research Letters 52(15): e2024GL113562. https://doi.org/10.1029/2024GL113562

Ramiadantsoa T, Stegner MA, Williams JW, Ives AR (2019) The potential role of intrinsic processes in generating abrupt and quasi-synchronous tree declines during the Holocene. Ecology 100(2): e02579. https://doi.org/10.1002/ecy.2579

Ray-Cozzens T (2022) Water-level changes in small lakes along the southern glacial margin of east-central North America during the late-Quaternary. Master's Thesis. University of Wyoming.

Reber EJ (1973) Soil survey, Susquehanna County, Pennsylvania. U.S. Department of Agriculture, Soil Conservation Service.

Reimer PJ, Austin WEN, Bard E, Bayliss A, Blackwell PG, Ramsey CB, Butzin M, Cheng H, Edwards RL, Friedrich M, Grootes PM (2020) The IntCal20 Northern Hemisphere radiocarbon age calibration curve (0–55 cal kBP). Radiocarbon 62: 725–757. https://doi.org/10.1017/RDC.2020.41

Schlenker N, Johnson J, Ray-Cozzens T, Nelson DM, Shuman BN, Stefanova I, Williams JW (2024) Interacting effects of fire and hydroclimate on oak and beech community prevalence in the southern Great Lakes region. Journal of Ecology 112: 1101–1122. https://doi.org/10.1111/1365-2745.14289

Seddon AW, Macias-Fauria M, Willis KJ (2015) Climate and abrupt vegetation change in northern Europe since the last deglaciation. The Holocene 25: 25–36. https://doi.org/10.1177/0959683614556383

Sevon WD (2000) Physiographic provinces of Pennsylvania, DCNR Map 13.

Sevon WD, Braun DD (1997) Glacial deposits of Pennsylvania, DCNR Map 59.

Shane LCK (1989) Changing palynological methods and their role in three successive interpretations of the late glacial environments at Bucyrus Bog, Ohio, USA. Boreas 18: 297–309. https://doi.org/10.1111/j.1502-3885.1989.tb00404.x

Shuman B (2003) Controls on loss-on-ignition variation in cores from two shallow lakes in the northeastern United States. Journal of Paleolimnology 30: 371–385. https://doi.org/10.1023/B:JOPL.0000007226.68831.e3

Shuman B, Newby P, Huang Y, Webb III T (2004) Evidence for the close climatic control of New England vegetation history. Ecology 85: 1297–1310. https://doi.org/10.1890/02-0286

Shuman BN (2024) Patterns of centennial to millennial Holocene climate variation in the North American mid-latitudes. Climate of the Past 20: 1703–1720. https://doi.org/10.5194/cp-20-1703-2024

Shuman BN (2025) Pollen records, postglacial, northeastern North America. In: Elias S (Ed.) Encyclopedia of Quaternary Science. Third Edition. Elsevier, Oxford, 541–552. https://doi.org/10.1016/B978-0-323-99931-1.00230-0

Shuman BN, Burrell SA (2017) Centennial to millennial hydroclimatic fluctuations in the humid northeast United States during the Holocene. Quaternary Research 88: 514–524. https://doi.org/10.1017/qua.2017.62

Shuman BN, Marsicek J, Oswald WW, Foster DR (2019) Predictable hydrological and ecological responses to Holocene North Atlantic variability. Proceedings of the National Academy of Sciences 116: 5985–5990. https://doi.org/10.1073/pnas.1814307116

Shuman BN, Newby P, Donnelly JP (2009) Abrupt climate change as an important agent of ecological change in the Northeast U.S. throughout the past 15,000 years. Quaternary Science Reviews 28: 1693–1709. https://doi.org/10.1016/j.quascirev.2009.04.005

Shuman BN, Stefanescu IC (2025) North American "warming holes" and European heat during abrupt Holocene cooling events in the Atlantic. Nature Communications 16: 9057. https://doi.org/10.1038/s41467-025-63330-4

Shuman BN, Stefanescu IC, Grigg LD, Foster DR, Oswald WW (2023) A millennial-scale oscillation in latitudinal temperature gradients along the western North Atlantic during the mid-Holocene. Geophysical Research Letters 50(20): e2022GL102556. https://doi.org/10.1029/2022GL102556

Stefanescu IC, Shuman BN, Grigg LD, Bailey A, Stefanova V, Oswald WW (2023) Weak precipitation δ^2H response to large Holocene hydroclimate changes in eastern North America. Quaternary Science Reviews 304: 107990. https://doi.org/10.1016/j.quascirev.2023.107990

Stefanescu IC, Shuman BN, Tierney JE (2021) Temperature and water depth effects on brGDGT distributions in sub-alpine lakes of mid-latitude North America. Organic Geochemistry 152: 104174. https://doi.org/10.1016/j.orggeochem.2020.104174

Sugita S (1993) A model of pollen source area for an entire lake surface. Quaternary Research 39: 239–244. https://doi.org/10.1006/qres.1993.1027

Thompson JR, Carpenter DN, Cogbill CV, Foster DR (2013) Four centuries of change in northeastern United States forests. PLoS ONE 8(9): e72540. https://doi.org/10.1371/journal.pone.0072540

Thompson RS, Anderson KH, Bartlein PJ (1999) Atlas of relations between climatic parameters and distributions of important trees

and shrubs in North America. U.S. Geological Survey Professional Paper 1650-B, Denver. https://doi.org/10.3133/pp1650AB

Toney JL, Rodbell DT, Miller NG (2003) Sedimentologic and palynologic records of the last deglaciation and Holocene from Ballston Lake, New York. Quaternary Research 60: 189–199. https://doi.org/10.1016/S0033-5894(03)00093-0

Turner MG, Baker WL, Peterson CJ, Peet RK (1998) Factors influencing succession: Lessons from large, infrequent natural disturbances. Ecosystems 1: 511–523. https://doi.org/10.1007/s100219900047

Turner MG, Braziunas KH, Hansen WD, Harvey BJ (2019) Short-interval severe fire erodes the resilience of subalpine lodgepole pine forests. Proceedings of the National Academy of Sciences 116: 11319–11328. https://doi.org/10.1073/pnas.1902841116

Turner MG, Romme WH, Gardner RH, O'Neill RV, Kratz TK (1993) A revised concept of landscape equilibrium: Disturbance and stability on scaled landscapes. Landscape Ecology 8: 213. https://doi.org/10.1007/BF00125352

Tzedakis PC (1992) Effects of soils on the Holocene history of forest communities, Cape Cod, Massachusetts, U.S.A. Géographie physique et Quaternaire 46: 113–124. https://doi.org/10.7202/032892ar

Umbanhowar CE (2004) Interaction of fire, climate and vegetation change at a large landscape scale in the Big Woods of Minnesota, USA. The Holocene 14: 661–676. https://doi.org/10.1191/0959683604hl745rp

USDA Natural Resources Conservation Service (2016) USDA-NRCS Official Soils Series Descriptions.

Watts WA (1979) Late Quaternary vegetation of central Appalachia and the New Jersey coastal plain. Ecological Monographs 49: 427–469. https://doi.org/10.2307/1942471

Webb III T (1986) Is vegetation in equilibrium with climate? How to interpret late-Quaternary pollen data. Vegetatio 67: 75–91. https://doi.org/10.1007/BF00037359

Whitmore J, Gajewski K, Sawada M, Williams JW, Shuman B, Bartlein PJ, Minckley T, Viau AE, Webb III T, Shafer S, Anderson P (2005) Modern pollen data from North America and Greenland for multi-scale paleoenvironmental applications. Quaternary Science Reviews 24: 1828–1848. https://doi.org/10.1016/j.quascirev.2005.03.005

Willard DA, Bernhardt CE, Korejwo DA, Meyers SR (2005) Impact of millennial-scale Holocene climate variability on eastern North American terrestrial ecosystems: pollen-based climatic reconstruction. Global and Planetary Change 47: 17–35. https://doi.org/10.1016/j.gloplacha.2004.11.017

Williams JW, Blois JL, Shuman BN (2011) Extrinsic and intrinsic forcing of abrupt ecological change: case studies from the late Quaternary. Journal of Ecology 99: 664–677. https://doi.org/10.1111/j.1365-2745.2011.01810.x

Williams JW, Post DM, Cwynar LC, Lotter AF, Levesque AJ (2002) Rapid and widespread vegetation responses to past climate change in the North Atlantic region. Geology 30: 971. https://doi.org/10.1130/0091-7613(2002)030%253C0971:RAWVRT%253E2.0.CO;2

Williams JW, Shuman B, Bartlein PJ, Whitmore J, Gajewski KJ, Sawada MC, Minckley T, Shafer S, Viau AE, Webb III T, Anderson PM, Brubaker LB, Whitlock C, Davis OK (2006) An Atlas of Pollen-Vegetation-Climate Relationships for the United States and Canada. American Association of Stratigraphic Palynologists Foundation, Dallas, TX.

Wood PO, McKee JM, Skemp LN, Nissley WB, Dickey JBR (1911) Soil survey of Bradford County, Pennsylvania. US Bureau of Soils.

Yu Z, McAndrews JH, Eicher U (1997) Middle Holocene dry climate caused by change in atmospheric circulation patterns: Evidence from lake levels and stable isotopes. Geology 25: 251–254. https://doi.org/10.1130/0091-7613(1997)025%253C0251:MHDCCB%253E2.3.CO;2

Zhao Y, Yu ZC, Zhao C (2010) Hemlock (*Tsuga canadensis*) declines at 9800 and 5300 cal yr BP caused by Holocene climatic shifts in northeastern North America. The Holocene 20: 877–886. https://doi.org/10.1177/0959683610365932